

5-5-2012

# Advanced Design Optimization for Composite Structure: Stress Reduction, Weight Decrease and Manufacturing Cost Savings

Shayan Ahmadian  
sha06001@engr.uconn.edu

---

## Recommended Citation

Ahmadian, Shayan, "Advanced Design Optimization for Composite Structure: Stress Reduction, Weight Decrease and Manufacturing Cost Savings" (2012). *Master's Theses*. 291.  
[https://opencommons.uconn.edu/gs\\_theses/291](https://opencommons.uconn.edu/gs_theses/291)

This work is brought to you for free and open access by the University of Connecticut Graduate School at OpenCommons@UConn. It has been accepted for inclusion in Master's Theses by an authorized administrator of OpenCommons@UConn. For more information, please contact [opencommons@uconn.edu](mailto:opencommons@uconn.edu).

**Advanced Design Optimization for Composite Structure:  
Stress Reduction, Weight Decrease and Manufacturing Cost Savings**

**Shayan Ahmadian**

B.A., University of Connecticut, 2010

A Thesis

Submitted in Partial Fulfillment of the

Requirements for the degree of

Master of Science

at the

University of Connecticut

2012

Master of Science Thesis

Advanced Design Optimization for Composite Structure:  
**Stress Reduction, Weight Decrease and Manufacturing Cost Savings**

**Presented by**  
**Shayan Ahmadian, B.A.**

Major Advisor.....

Eric Jordan, PhD

Associate Advisor.....

Montgomery Shaw, PhD

Associate Advisor.....

Wei Sun, PhD

University of Connecticut  
2012



## Contents

List of figures .....	v
List of tables .....	vii
Abstract.....	viii
1. Introduction .....	1
1.1. Project approach.....	1
1.2. Composite and Its Application .....	3
1.3. Hydraulic Actuator and functionality.....	6
1.4. Specifications for hydraulic actuator .....	6
2. Material Selection .....	7
3. Design consideration.....	11
3.1. Structural configuration .....	11
3.1.1. Long tension rods.....	11
3.1.2. Flange mounted covers.....	13
3.1.3. Glued On Flanges .....	13
3.1.4. Threaded Covers .....	14
3.2. Short Fiber.....	15
3.3. Long Fiber.....	15
3.3.1. Wound Tube.....	15
3.3.2. Braided Tube .....	16
4. Finite Element Analysis of Enclosure parts (Bonded contacts).....	17
4.1. Geometry .....	17
4.2. Mesh .....	18
4.3. Loads and boundary conditions.....	21
4.4. Solver algorithm.....	22
4.5. Stress evaluation in enclosure parts .....	22
5. Finite Element Analysis of Piston Assembly.....	25
5.1. Geometry .....	25
5.2. Mesh .....	26
5.3. Loads and Boundary conditions for compression mode .....	27
5.4. Loads and Boundary conditions for tension mode .....	30
5.5. Solver's Algorithm for buckling.....	32

5.6.	Compression mode stress evaluation .....	32
5.7.	Piston assembly under buckling.....	37
5.8.	Tension mode stress evaluation .....	39
6.	Failure Criteria.....	41
6.1.	Static Structural.....	42
6.2.	Buckling.....	42
6.3.	Creep.....	43
6.4.	Fatigue.....	44
7.	Stress Reduction by shape optimization.....	45
8.	Weight Decrease by shape optimization .....	48
9.	Manufacturing Cost Savings.....	49
10.	Risk Assessment .....	53
10.1.	Surface Wear .....	53
10.2.	Water absorption.....	57
11.	Summary .....	57
	Work Cited .....	59

## List of figures

Figure 1	Clevis mount hydraulic actuator .....	6
Figure 2	Tensile strength of reinforced TORLON vs. other comparable reinforced resins at 400F.....	10
Figure 3	Creep resistance performance for TORLON 5030 at 400°F .....	10
Figure 4	Long tension rod design: from left to right: $P_2 \gg P_1$ , $P_1 \gg P_2$ and $P_1 = P_2 = 0$ maximum buckling .	12
Figure 5	Long tension rod design concept exploded and unexploded view.....	12
Figure 6	Flange mount design: from left to right $P_2 \gg P_1$ , $P_1 \gg P_2$ , $P_1 = P_2 = 0$ no buckling .....	13
Figure 7	Wound tube concept .....	16
Figure 8	Simplified geometry of the enclosure parts for static structural FEA.....	18
Figure 9	Mesh for Bonded contact FEA .....	19
Figure 10	Mash metrics for enclosure assembly of Bonded Contact Analysis .....	20
Figure 11	High jacobian ratio elements highlighted in cyliner assembly for bonded contact FEA .....	20
Figure 12	Boundary condition for Bonded contact FEA.....	21
Figure 13	Surfaces in which pressure is applied to, cross section view.....	22
Figure 14	Von mises equivalent stress for enclosure parts of bonded contact FEA under proof loading(full) .....	23
Figure 15	Von mises equivalent stress for enclosure parts of bonded contact FEA under proof loading (cross-section).....	24
Figure 16	From left to right; Fully contracted, Half way and Fully extended .....	26

Figure 17 Mesh for the piston, from left to the right; contracted, halfway and fully extended with average jacobian ration of 3.29, 3.29 ,3.29 .....	27
Figure 18 Boundary conditions for the piston in compression mode and buckling .....	29
Figure 19 Loads for the piston in compression mode and buckling .....	29
Figure 20 Boundary conditions for the piston in tension mode .....	31
Figure 21 Loads for the piston in tension mode .....	31
Figure 22 Von mises stress for the piston under proof loading in contracted mode .....	35
Figure 23 Von mises stress for the piston under proof loading in half way mode .....	36
Figure 24 Von mises stress for the piston under proof loading in fully extended mode .....	37
Figure 25 exaggerated modal displacement for proof loading: from left to right; Fully contracted, Half way and Fully extended .....	39
Figure 26 Von mises stress for piston in tension mode under proof loading.....	40
Figure 27 High temperature flexural fatigue strength of TORLON resin at 350F, 30Hz .....	45
Figure 28 First simplified 2D model with flat Front/Back Cover in glued on configuration demonstrating the stress in endcap being 156ksi at 2130psi .....	47
Figure 29 Optimized dome shaped Front/Back Cover in flange mount configuration with highest stress being 22.5ksi at 2130psi.....	48
Figure 55 Injection molding quote for TORLON parts presented by Aztec Plastic, Inc. ....	51
Figure 56 Actuator in full stroke .....	56
Figure 57 Force equilibrium diagram on piston for calculating the reaction forces caused by the side load .....	56
Figure 33 The prototype TORLON actuator. Cylinder is machined from extruded TORLON rod, Piston is injection molded. Front and Back Cover are machined from Aluminum due to low budget.....	59

## List of tables

Table 1 Candidate materials .....	8
Table 2 Properties of Masterbond epoxy, EP 41S-1HT. Courtesy of Masterbond® .....	14
Table 3 Pull out strength for TORLON Resin .....	14
Table 4 Buckling load factor for proof and working loading.....	38
Table 14 Complete part list with weights and weight savings for TORLON actuator .....	49
Table 15 Cost analysis for TORLON actuator based on 3,000EAU .....	52
Table 16 Projected surface area for parts subjected to wear .....	56



## Abstract

*An injection moldable chopped fiber composite actuator with detailed drawing and tolerances was designed within one year. A vendor was selected and a quote for injection molding tooling cost for production was obtained and the first prototype was built in addition of six months. The risks are identified and material characterization tests are proposed.*

*The objective of this project was redesigning an aluminum made actuator with a continuous fiber composite for weight saving purposes. After searching the literature and consulting with experts in the field it was concluded that manufacturing costs associated with continuous fiber composite are 3 times as much and weight savings are 40-60%. At this point project got shifted to a new direction.*

*Instead of continuous fiber, chopped fiber composite was selected, namely TORLON 5030 which is a PIA with 30% glass filler. TORLON 5030 is injection moldable which reduces the manufacturing costs associated with the machining of the current aluminum made actuator by a 92%. However the specific strength of TORLON 5030 is lower than aluminum by 20%. This means that the chopped fiber actuator would weigh if not more at least the same as aluminum actuator. In order to reduce the weight shape optimization was applied. After 12 revisions of FEA integrated with CAD stress was reduced by a factor of 10 and weight was decreased by a factor of 4.*

# 1. Introduction

## 1.1. Project approach

Before embarking on the details and technical work done in this project it is worth mentioning the project initiation, the approach taken in new technology development and key factors in which made this project successful. This project initiated in January 2010 with the objective requested by the sponsor “replacing aluminum in current actuator with a composite to reduce weight”. The type of composite and possible redesign of actuator was not specified.

After extensive research reviewing the literature, internet, journals and consulting with professors and industrial leaders in composites and engineering plastics it was concluded that there are no structural plastics that could replace aluminum for weight savings at above 300°F because specific strength of Aluminum at 300°F is higher than all commercially available plastics. In fact there are only two polymers that have glass transition temperatures above 300°F which are mentioned in section 2 Material Selection.

In the early stages the type of composite most applicable for actuator was unclear. The focus began by studying long fiber composite, primarily wound and braided. It quickly became apparent that the study of long fiber composite for a complicated geometry, such as an actuator which has moving parts and many discontinuities at the location of flange, hydraulic inlet/outlet piston opening and front/back cover, is very complicated, expensive in terms of manufacturing and time consuming. Since the primary goal of this project was money savings and funds were limited to 2 years with delivering a fully functional actuator the study of long fiber composite for actuator was not promising.

An examination of the current actuators was done to understand the functionality of the actuator, the critical mechanical failure modes and the current processes of manufacturing the aluminum

actuator. The major cost of a current actuator is associated with machining. The current actuator is machined from a block of aluminum and costs about \$3,500 due to the intricate geometry. Since further machining would bring additional manufacturing costs, the current actuator is made bulkier than needed. Therefore, time weight reduction was not the primary goal, or Finite Element was not a very robust tool for design optimization.

Consequently the project shifted to a new direction. It was determined that the best candidate composite would be an injection moldable short fiber composite that can be used as a structural material for operating temperature of 300°F. After evaluating a various structural configurations, creep is identified as the limiting design factor. The discussion of these structural configurations can be found in Section 3. Design consideration.

Following the selection of the best structural design, a series of 12 revisions of FEA integrated with CAD produced a stress reduction by a factor of 10. This shape optimization is the key element that reduced the weight by a factor of 5, otherwise specific strength of aluminum is higher than that of composite. The outcome of this work demonstrates an actuator from injection molding the optimized shape would lead to the resulting aluminum made actuator to weigh less than the composite one. However injection molding of the composite that we carefully selected is much faster and less expensive than casting an aluminum one. The details of shape optimization and weight reduction can be found in Section 7. Stress Reduction by shape optimization and 8. Weight Decrease by shape optimization.

## 1.2.Composite and Its Application

A composite material consists of two or more separable materials which are combined in a macroscopic structural unit (Gibson, 1994). The main advantage of using a composite structural material compared to other structural materials such as metals, ceramics or polymers, is that the specific strength (the ratio of tensile strength to density) of composites is much higher. Thus in applications such as aircraft or spacecraft where weight reduction is important, composites can play a significant role. Beside strength and weight, there are other properties that can be improved by forming a composite such as (Jones, 1975);

- Stiffness
- Thermal expansion
- Corrosion resistance
- Fatigue life
- etc.
- Temperature dependent properties
- Wear resistance

Composites are classified in three main categories (Jones, 1975);

- Fibrous composites which consists of fibers in a matrix.
- Laminated composites which consist of layers of various materials.
- Particulate composites which composed of particles in a matrix.

The scope of this paper is limited to fibrous composites only. Fibrous reinforcement is so effective because many materials are much stronger and stiffer in fiber form than they are in bulk form. The smaller the diameter of the fiber, the smaller likelihood that failure inducing surface cracks would be generated during fabrication and handling. However fibers alone cannot support any compressive force and their transverse properties are unfavorable as they are longitudinal. Thus fibers are undesired

as structural material unless they are held together in a structural unit by a matrix (Gibson, 1994). The matrix is basically a binder that generally is weaker and lighter than the fibers but provides support in transverse direction and prevents fibers from buckling by taking the compressive force.

The need for fiber placement in different orientation diversifies the class of fibrous composites in four main groups;

- Long fiber composite; Continuous fiber composite and Woven fiber composite
- Chopped fiber composite
- Hybrid composite

The long fiber composite is widely used because they have higher specific strength compared to chopped fiber composite. In continuous fiber composites fibers are placed straight in a plane to form a lamina and laminae are oriented and bonded by the matrix in the required directions. Although continuous fiber composite is extensively used, delamination is the major problem in continuous fiber composite (Gibson, 1994). This delamination is the separation of the laminae by the interlaminar shear between each lamina which dominated by shear strength of the matrix.

The matrix for the fibrous composite is normally is a polymer. Polymers are classified as either thermoset or thermoplastics. Examples of thermosets are epoxy, polyester and phenolic or thermoplastics. Thermoplastics include polyimide (PI), polysulfone (PS), polyetheretherketone (PEEK) and polyphenylene sulfide (PPS). Upon curing thermosets form a highly cross linked, three dimensional molecular network which does not melt at high temperature. Thermoplastics however are based on polymer chains which do not cross link. As a result thermoplastics will soften and melt at high temperature and then harden again upon cooling (Gibson, 1994).

One practice in eliminating delamination in fabrication of long fiber composite is woven fiber composite. Consequently since the fibers are not oriented straight, strength and stiffness are sacrificed. Also, fabrication costs of woven fiber composite increases significantly, as well as requiring a significant investment in design. . Chopped fiber composites are also susceptible to delamination and their manufacturing costs are incredibly cheaper since parts can be molded (Gibson, 1994). In chopped fiber composites, fibers may be randomly oriented but with the right mold design, orientation of the fibers can be controlled. Chopped fiber composite can have between thirty to forty percent fibers and obtain strength of thirty to forty kpsi.

Fibers and matrix must be chemically compatible so that any undesirable chemical reaction would not occur at the interface and also bond well together. There are different types of fibers such as glass fibers, carbon fibers, Aramid fibers, silicon carbide fibers, aluminum and steel fibers. ????? shows the properties of some of the commercially available fibers. Carbon fiber and glass fiber are widely used in advanced composites. When a single fiber material does not have all the desired properties, hybrid composite consisting of two or more fiber material can be used.

Composite structures are widely used nowadays in variety of components for automotive, aircraft, marine and even in consumer products such as golf, ski, and tennis. Military aircraft designers were among the first to realize the importance of composites for weight reduction since performance of these vehicle heavily depend on weight. Examples of aircrafts with composite components are Boeing 757 and 767 where most of the body, wing and empennage are made out of long fiber and woven composite. Although composite have been used for a variety of aircraft parts, yet they have not been used for engine components due to their temperature and fuel exposure limitation (Gibson, 1994).

### 1.3. Hydraulic Actuator and functionality

A Hydraulic Actuator is an incompressible fluid driven resembling a piston-cylinder structure that transforms a linear motion via the piston. This transition of linear motion is used to actuate a valve or gate by opening or closing it. Hydraulic actuators come in different mounting configuration and pressure ratings. In order to favor the chance of success in this project, a hydraulic actuator with smaller pressure rating (2130psi) and cover-face-to-wall mount configuration has been considered. In this design end caps or “front cover” and “back cover” are used to contain the pressure and front cover is face mounted to a plate. This design is introduced in later sections. Figure 2 shows a clevis mount hydraulic actuator.

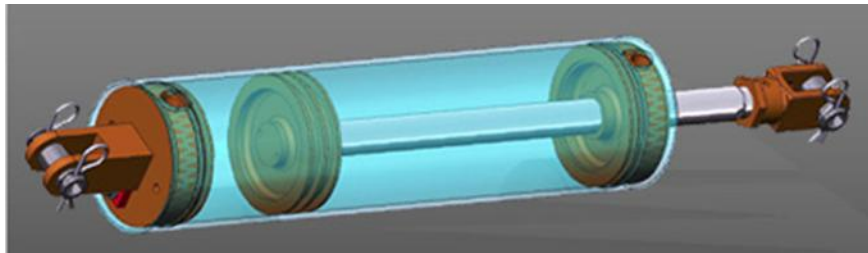


Figure 2 Clevis mount hydraulic actuator

### 1.4. Specifications for hydraulic actuator

The actuator operates at 300°F, 211psi and 1Hz. However the actuator must be designed in a way that it can survive a surge load due to pump malfunction. In case of a surge load actuator must be able to withstand a proof pressure of 2130psi and a 30lb side load when in full stroke.

## 2. Material Selection

The candidate material must be commercially available and easily manufactured at reasonable costs. In addition must have the following traits:

- *Glass Transition Temperature( $T_g$ )* above 300F
- *Specific strength* close or better than aluminum at 300F
- *Mechanical fatigue* life of 100M cycles at 5ksi for maximum 3Hz
- *Coefficient of Thermal Expansion(CTE)* close to aluminum
- *Creep* resistance at 300F and 5ksi
- Good surface wear properties
- Low water absorption and dimensional changes

After extensive research, it was determined that no single polymer has all the traits listed. Also there is no manufacturer that has specified all the characteristics for the material properties needed for this project. Since the primarily use of this device is structural, a list of all possible candidates based on specific strength at 300F was gathered. Then the list was filtered upon other requirements and at the end availability and cost. Such a list can be found in Table 1. This table was last update on August 2011.



Material		Glass Transition Temperature (F)	Tensile Strength (Kpsi)	Tensile Elongation (%)	CTE (PPM/F)	Density (lb/in <sup>3</sup> )	Tensile Modulus (Kpsi)	Specific Strength (Kpsi/lb/in <sup>3</sup> )
Current material	Al 2024	N/A	68	19	12.9	0.100	10600	680
	AISI 4340	N/A	68.2	22	6.83	0.284	29700	240
Long Fibers	Carbon fiber TC-42	N/A	710	1.7	2.5	0.065	42000	10923
	Kevlar 49	320	525	3.5	-2.7	0.052	16300	10096
	Typical Carbon fiber tube-TC33	350	275	1.7	6	0.056	17000	4911
Short Fiber Composite	Graphite Phthalonitrile Composite	842	351	1.4		0.074	23496	4763
	AMC 8590	245	41			0.053	8000	767
	HiFill PEEK CF40 HF	250	40	1.5	6	0.052	4400	764
	Victrix Peek 450CA30	275	30	1.7	6	0.051	2900	593
	Torlon 5030	500	29.4	6	9	0.053	3230	551

Table 1 Candidate materials

Looking at Table 1 it is clear that only long fiber composites have specific strength higher than aluminum. After consulting with experts in the field of composite fabrications both in academia and industry it was concluded that if long fiber composite is chosen the manufacturing costs would increase by a factor of 3 and there would be 40 to 60 percent weight savings. It was also concluded that if chopped fiber composite is used there may not be any weight savings because the specific strength of chopped fiber composites are lower than aluminum at 300°F. However one advantage of chopped fiber composites are the injection molding. If an injection moldable chopped fiber can be identified that has glass transition temperature above 300F and specific strength close to aluminum at 300F, the manufacturing costs would decrease dramatically. Also, shape optimization can be applied to reduce

the weight since any complex geometry can be achieved with a little or no extra cost with injection molding. Thus at this point project got shifted to a new direction. Instead of long fiber composite which the sponsor suggested, the chopped fiber composite was identified as the best material for this project.

Examining Table 1 again, it is clear that there are not many engineering plastics that have glass transition temperature above 300°F. Graphite Phthalonitrile is a chopped fiber composite developed by Navy's Research Laboratory and has outstanding properties that are promising the possibility of development of the actuator. However it is not commercially available yet. Most commercially available chopped fiber composites have a tensile strength of approximately 30 to 40 ksi with 30%-40% chopped carbon fiber as reinforcement respectively. However not many high temperature resins work at a temperature of 300F.

It was concluded that TORLON resin has the highest Tg. Figure 3 illustrates a comparison between the tensile strength of reinforced TORLON and other comparable reinforced resins at 400F. Because TORLON can be glass or carbon fiber filled, after further investigation TORLON with 30 percent chopped glass fiber, commonly known as TORLON 5030, was chosen because of the following;

- There are creep limitations in designing the actuator and TORLON 5030 undergoes almost 0% strain at 5ksi and 400F for 1000 hours, Figure 4.
- Using glass filled instead of carbon filled eliminates the *Galvanic Corrosion* issue.
- The glass filled TORLON has CTE closer to Al 2024 which reduces the polymer to metal interface thermal mismatch.

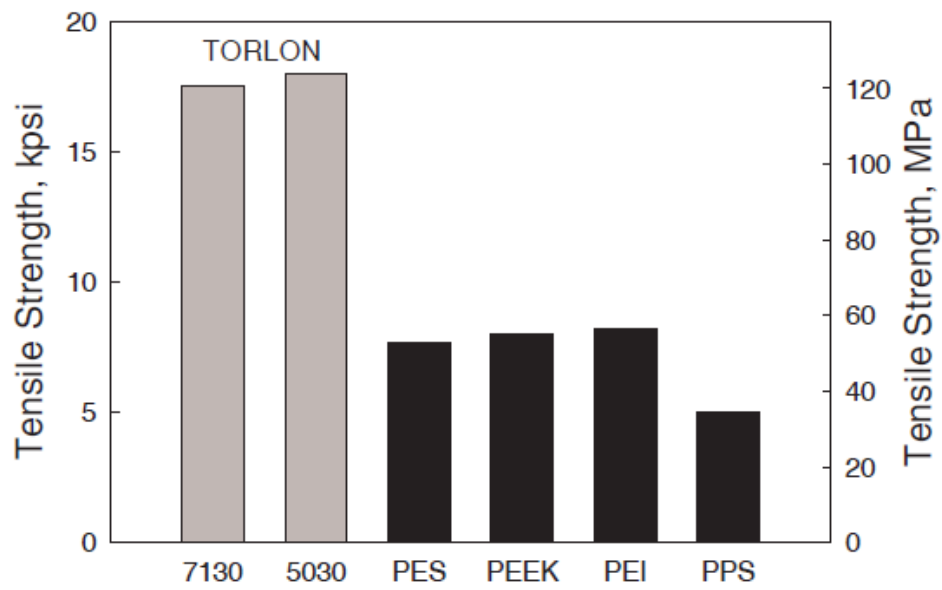


Figure 3 Tensile strength of reinforced TORLON vs. other comparable reinforced resins at 400°F

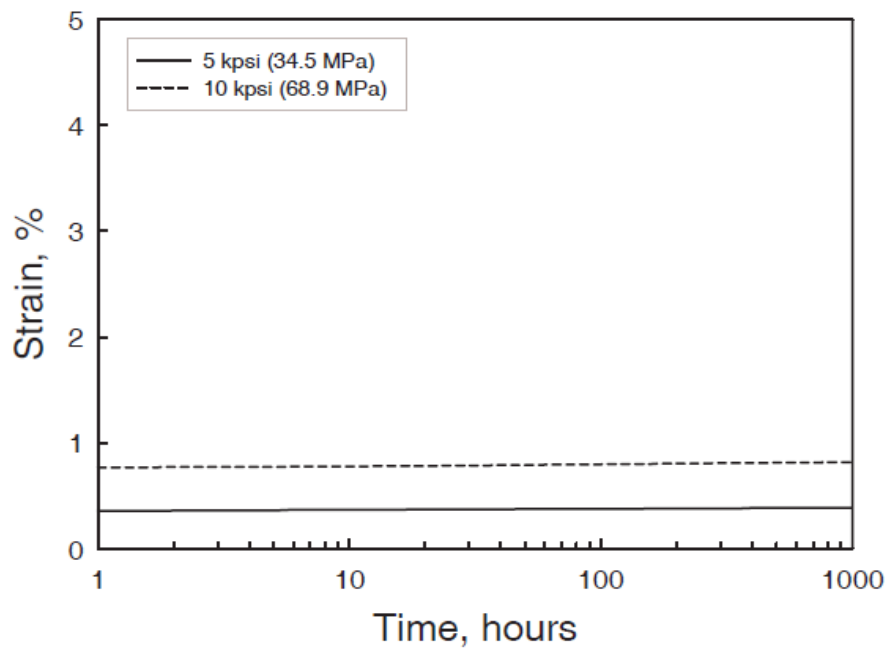


Figure 4 Creep resistance performance for TORLON 5030 at 400°F

### **3. Design consideration**

#### **3.1.Structural configuration**

##### **3.1.1. Long tension rods**

It was proposed to use two tension rods to attach the covers to the cylinder. Figure 6 shows this design concept. The mechanical failure modes considered for the tension rods are yielding and thermal mismatch. In order for the rods to prevent separation between covers and cylinder, rods must be tightened to a pretension bolt force of contaminating the proof pressure, thermal mismatch and seal force. This means bolts are in state of tension and the cylinder sees maximum compressive force when there is no internal pressure and at minimum temperature. When under such loadings the cylinder is subjected to buckling, Figure 5. In order to prevent the buckling the thickness of the cylinder must be increased to a value that not only brings no weight savings for the actuator but also increases the weight by 30% percent.

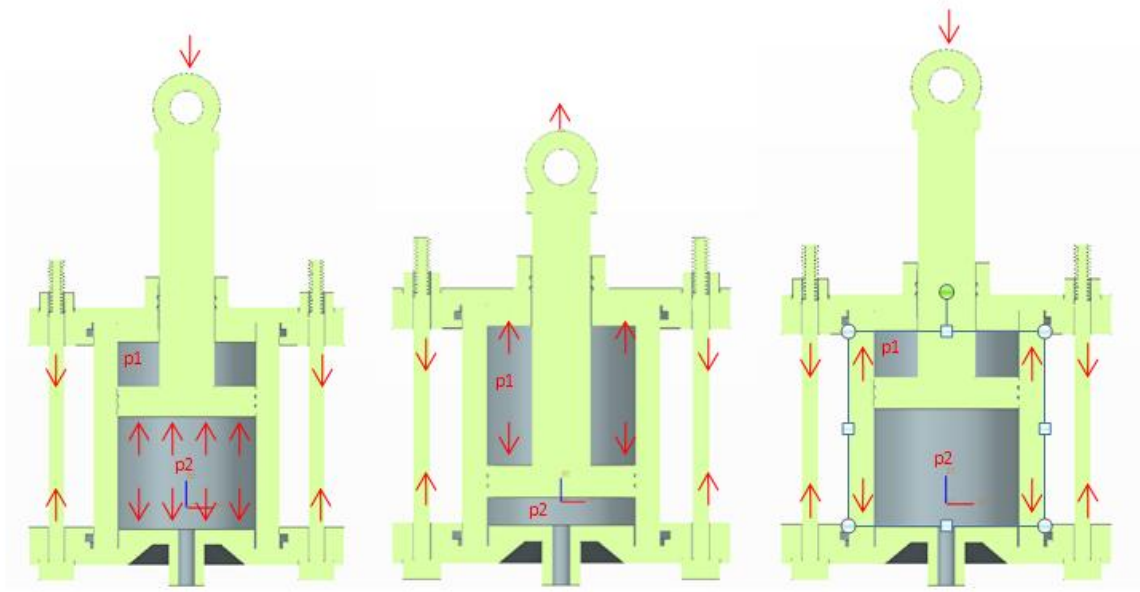


Figure 5 Long tension rod design: from left to right:  $P_2 \gg P_1$ ,  $P_1 \gg P_2$  and  $P_1 = P_2 = 0$  maximum buckling

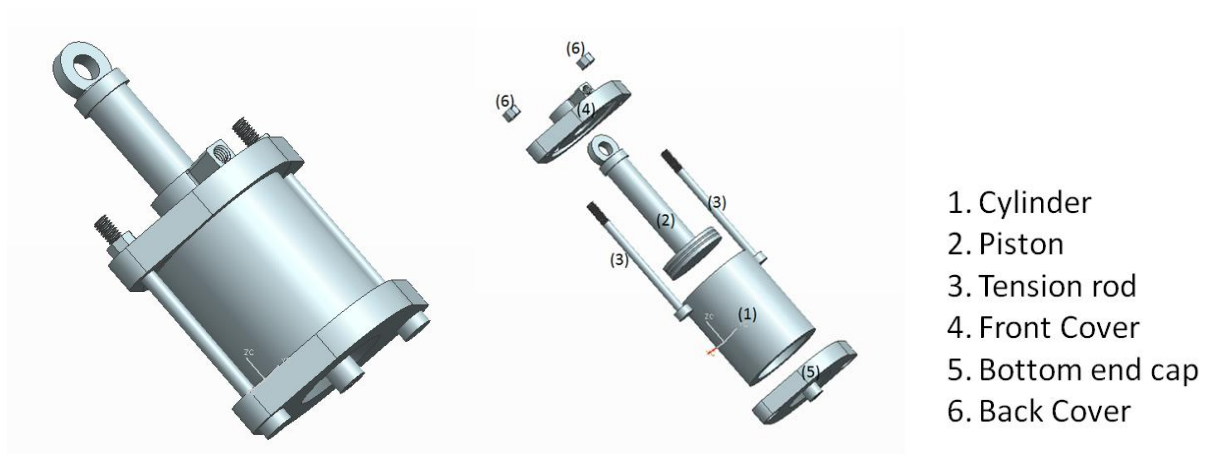


Figure 6 Long tension rod design concept exploded and unexploded view

### 3.1.2. Flange mounted covers

After realizing buckling produces the highest mechanical failure mode in the actuator for the “long tension rod” design mentioned above, a revision needed to be considered. Flanges are added to the cylinder and covers are bolted to the flanges as pictured in Figure 7. This design concept eliminates the buckling of cylinder completely and increases its weight savings to 70%.

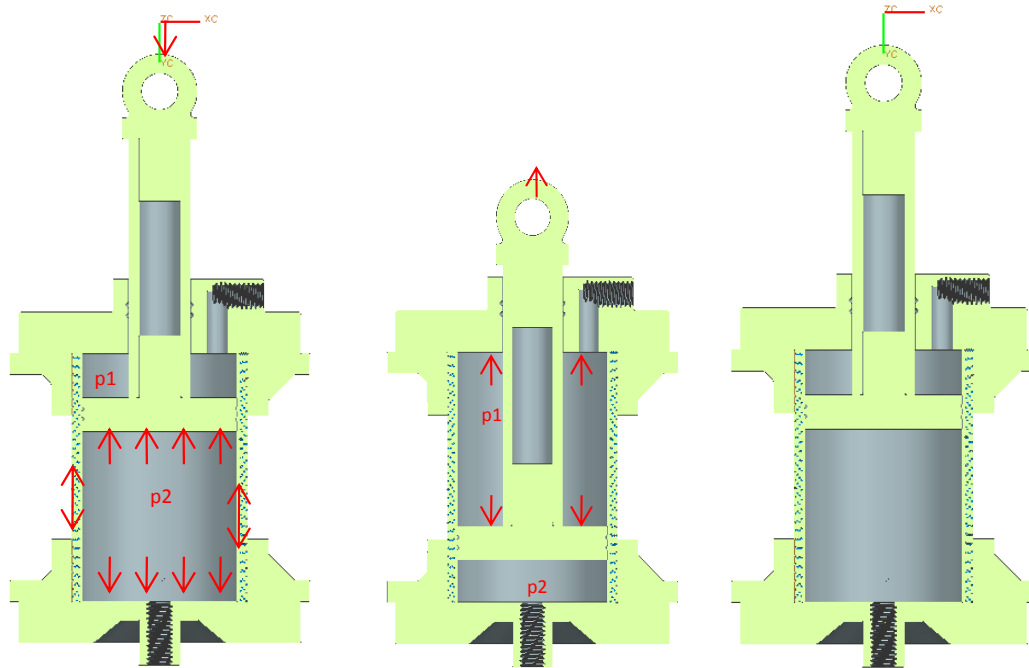


Figure 7 Flange mount design: from left to right  $P_2 \gg P_1$ ,  $P_1 \gg P_2$ ,  $P_1 = P_2 = 0$  no buckling

### 3.1.3. Glued On Flanges

For easier and faster manufacturing a long tube can be made by the means of extrusion, molding etc. The long tube then is cut to the appropriate length. Thus the flange has to be a separate piece. Flange can be attached to the cylinder by either recurring the matrix/resin or an epoxy. The most suitable epoxy that could withstand high shear stress at the design temperature range was found to be Masterbond epoxy, EP 41S-1HT is considered with properties shown in table 1. A simple hand

calculation revealed that the minimum bond length must be 0.25" to give a factor of safety of 2 at proof pressure.

Material	Operating Temperature (F)		Cure Schedule		Tensile Strength (Kpsi)	CTE (PPM/F)	Density (lb/in3)	Tensile Modulus (Kpsi)	Viscosity cPs
EP41S-1HT	-60	+350	200F	1-2hrs	10	50	N/A	450	60,000 to 100,000

Table 2 Properties of Masterbond epoxy, EP 41S-1HT. Courtesy of Masterbond®

#### 3.1.4. Threaded Covers

Another design concept considered is to attach the covers to the cylinder by the means of threading. Both internal and external threads can be molded using normal molding practices to Class 2 tolerance using TORLON resins. Class 3 can be molded using very high precision tooling. Table 3 shows the screw holding strength of TORLON threads for TORLON resin with no reinforcement. Holes were drilled for #4-40 screws and tapped in 0.19 inch (4.8mm) thick TORLON plaques. Screw pull-out strength determined by ASTM D1761. Note: it is assumed that in molded threads there will not be any chopped fiber reinforcement. A hand calculation has been done based on shear strength of TORLON for and the experimental data shown below are validated with 3% difference. The same approach is then applied for the threading definition required to fasten the covers to the cylinder. For an engagement length of 0.5 inches a factor of safety of 5 was achieved.

TORLON Grade	Pull out Strength (lb)	Number of Threads engaged
4203L	540	7.5

Table 3 Pull out strength for TORLON Resin

### 3.2.Short Fiber

It was assumed that with low stresses using long fiber composite is not feasible because the further weight savings would be offset by increasing manufacturing costs by a factor of 3. Thus the design of a short fiber composite such as TORLON 5030 where primary components can be manufactured by injection molding became the objective. Since the stresses induced by pressure in this model of actuator are very low (5ksi at proof pressure) using TORLON is more feasible due to lower fabrication costs.

### 3.3.Long Fiber

For bigger actuators considering long continuous fiber is more feasible to get high specific strength, keeping in mind fabrication costs increase and delamination remains as an issue.

#### 3.3.1. Wound Tube

The Simplest opportunity for long continuous carbon fiber is winding the pressure vessel. Winding the pressure vessel would prevent swelling when pressurized thus eliminating the internal leakage at high pressure. However the biggest challenge is thermal expansion mismatch. Long continuous fibers such as Carbon, Graphite or Kevlar have very low CTE as mentioned in Table 1. This thermal mismatch can yield high stresses in fiber. The stress in axial direction is;

- Stress in bolt:30,000psi
- Stress in graphite:14,570psi

In the Hoop Direction graphite has a large strain to failure so the design is limited by strain to failure of the liner. To make this big HIGH STRENGTH STEEL must be used as liner material.



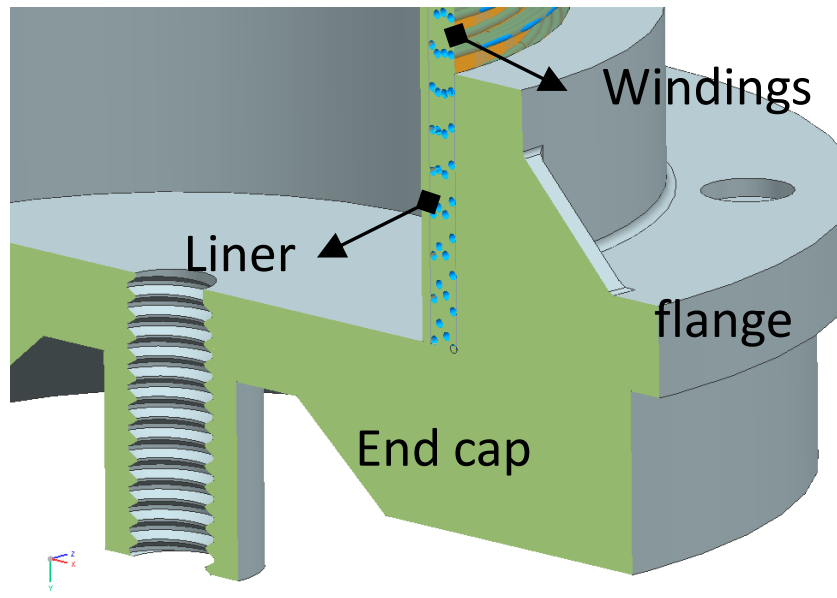


Figure 8 Wound tube concept

### 3.3.2. Braided Tube

As mentioned earlier, braiding will eliminate the delamination problem and increase specific strength by a factor of 10 as shown in Table 1. However the fabrication cost increases dramatically based on length and geometric complexity of the part. Pursuing braided tube for the 2300psi rated actuator would decrease the weight by only 0.3lb in comparison to short fiber composite and increase the manufacturing costs by a factor of 3. Thus it was realized for the current 2130psi rated actuator considering braided composite would not be economically feasible. However for the bigger actuators (10ksi and higher) braiding is suggested. Also, it is recommended to cover the short fiber composite actuator with Kevlar wrapping or a braided Kevlar sock to prevent it from swelling at high loads and also unexpected impacts such as explosion and bullets.

## 4. Finite Element Analysis of Enclosure parts (Bonded contacts)

### 4.1.Geometry

To examine the performance of the structure a finite element code (FEA) in ANSYS 12.1 is written.

First geometry is carefully simplified to reduce unwanted features without distorting the design concept.

The model is divided into two parts. Part one performs FEA on piston and Part two performs FEA on the enclosure parts for the piston such as cylinder, Back/Front Cover etc. The simplifications for the enclosure parts are;

- Threads removed from; bolts, nuts, hydraulic in/out lets.
- Bodies unified as one for bolt, washer and nut.
- Details removed from bolt head.

Figure 9 demonstrate the simplified geometry of the enclosure parts for static structural FEA. It is worth mentioning that parts are assembled in UGS NX 7.0 with proper constraints such aligning the axis of the Cylinder with Back/Front Cover and applying the touch constraint for mating surfaces of Washers to Cylinder flange, etc. Furthermore to make sure parts are assembled correctly, an interference analysis is performed in UGS NX 7.0.

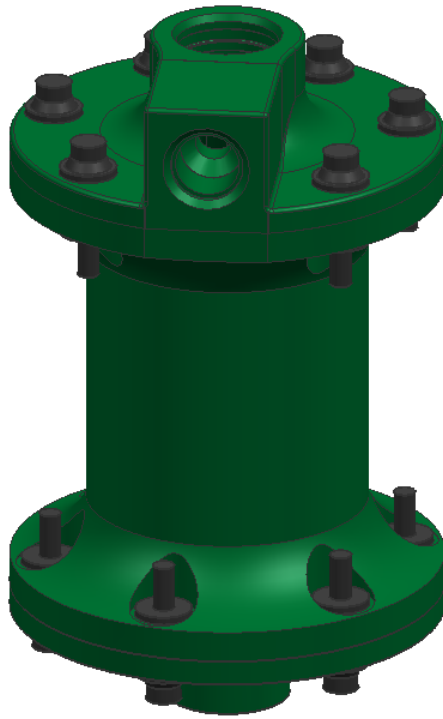


Figure 9 Simplified geometry of the enclosure parts for static structural FEA

#### 4.2.Mesh

Next the CAD model was imported into ANSYS 12.1. Due to complexity level of geometry the built-in automatic meshing algorithm of ANSYS 12.1 was used. The structural element type used here is SOLID187 which is a 3D 10-node tetrahedral structural solid element with UX, UY, UZ degrees of freedom and there are 1,373,502. Thus overall there are 1,976,934 nodes in the model. Figure 10 shows the mesh quality of this model.

Once the mesh was generated, mesh was checked for element distortion. The Jacobian Ratio is calculated as a method of mesh metric and the following parameters are obtained; minimum 1, maximum 39.947, mean 1.026, with a standard deviation of 0.486. Figure 11 shows the plot of distribution of Jacobian Ratio. Note that Jacobian Ratio is highly clustered around value of 2.29. In

order to make sure this small amount of distorted element will not bias the FEA result, the distorted elements are located. It was determined these distorted elements appear around sharp contours such as a sharp edge. Figure 12 highlights the elements with high Jacobian ratio. As it is demonstrated they are in no interested areas such as the drill end angle or edge on the ID of the cylinder. These elements are unstable and produce high stress. As long as there are few and not present in areas of interest, it is acceptable that model contains a few elements with high Jacobian ratio.

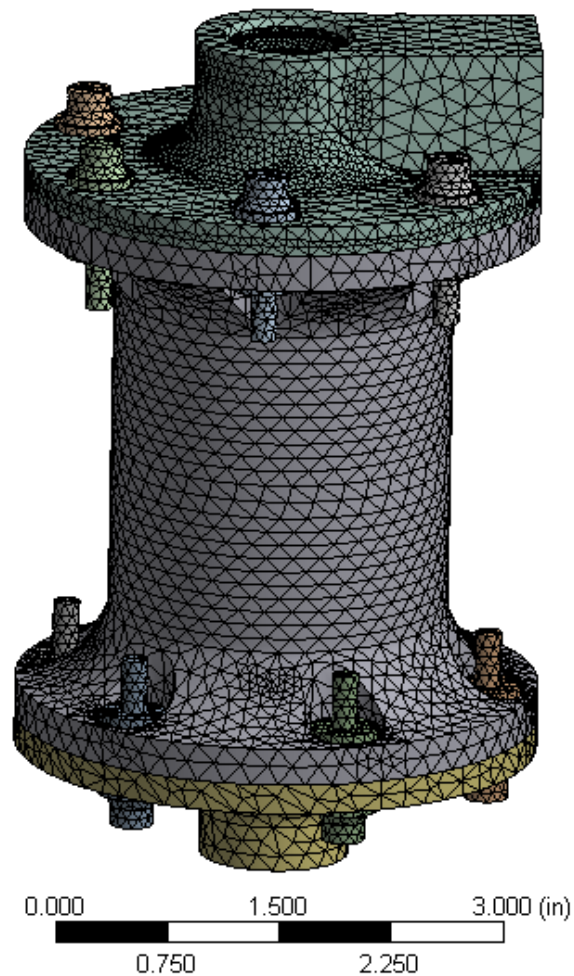


Figure 10 Mesh for Bonded contact FEA

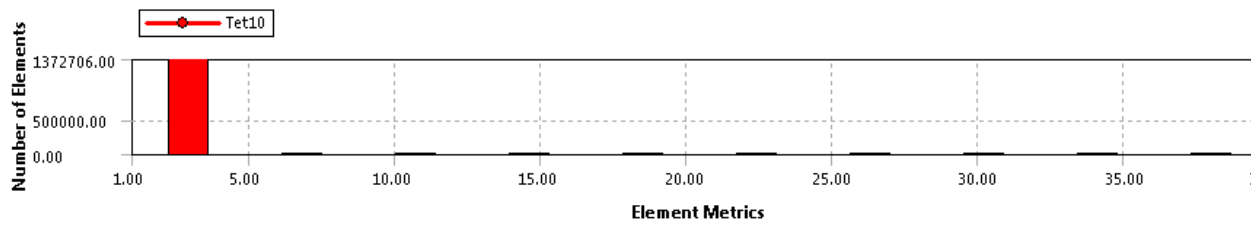


Figure 11 Mash metrics for enclosure assembly of Bonded Contact Analysis



Figure 12 High jacobian ratio elements highlighted in cyliner assembly for bonded contact FEA

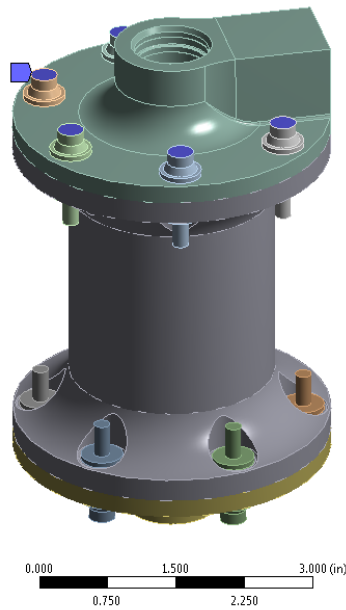
### 4.3.Loads and boundary conditions

After meshing is successfully done, loads and boundary conditions are applied. Since this prototype will be mounted on a plate that sits on the flange of Front Cover, Boundary conditions are such that; Flat face of bolt heads for the front cover are fixed in all degrees of freedom. The schematic of boundary condition is shown in Figure 13. After boundary conditions have been applied pressure is applied to all internal surfaces of Cylinder and Front/Back Cover. For the Bonded Contact FEA, stress is obtained for;

- Proof pressure
- Maximum working
- And Cruise pressure

Also, a temperature load of 300F is applied to all parts.

Fixed Support  
Time: 1. s  
1/27/2012 10:40 AM  
■ Fixed Support



ANSYS<sup>®</sup>  
Noncommercial use only

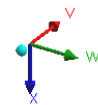


Figure 13 Boundary condition for Bonded contact FEA

A: Static Structural (ANSYS)  
Pressure  
Time: 1 s  
3/9/2012 2:30 PM  
■ Pressure: 211. psi

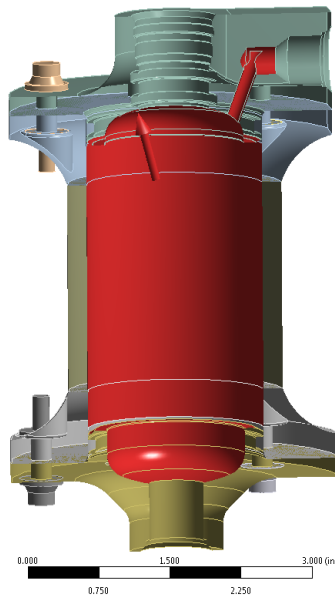


Figure 14 Surfaces in which pressure is applied to, cross section view

#### 4.4.Solver algorithm

Since there are no non-linearities other than geometry the direct solver is used. The analysis is done on a single processor at 2.8GHz requiring 3,421MB minimum memory and taking 00:12:18 to finish.

#### 4.5.Stress evaluation in enclosure parts

Once the simulation is successfully finished post processing is applied to extract the result. Figure 15 and Figure 16 show the normalized Von Mises for both full body and cross sectional view respectively under proof loading. Note the stress contours shown are very smooth which confirms that the model has reached equilibrium and converged. Even though reduced integration in elements has been avoided model was examined to make sure there is no hourglass effect. Another check is intuitively inspecting the stress contour. As Figure 15 and Figure 16 shows stress is higher around the location of bolts (bolt clamping force), stress contours for cylinder is uniform and the stress concentration around the radiuses are constant. All these qualitative checks support the results obtained. The stress in enclosure parts are kept below 5ksi under proof loading pressure of 2130psi and at 300°F. The maximum stress occurred in cylinder ID midsection.

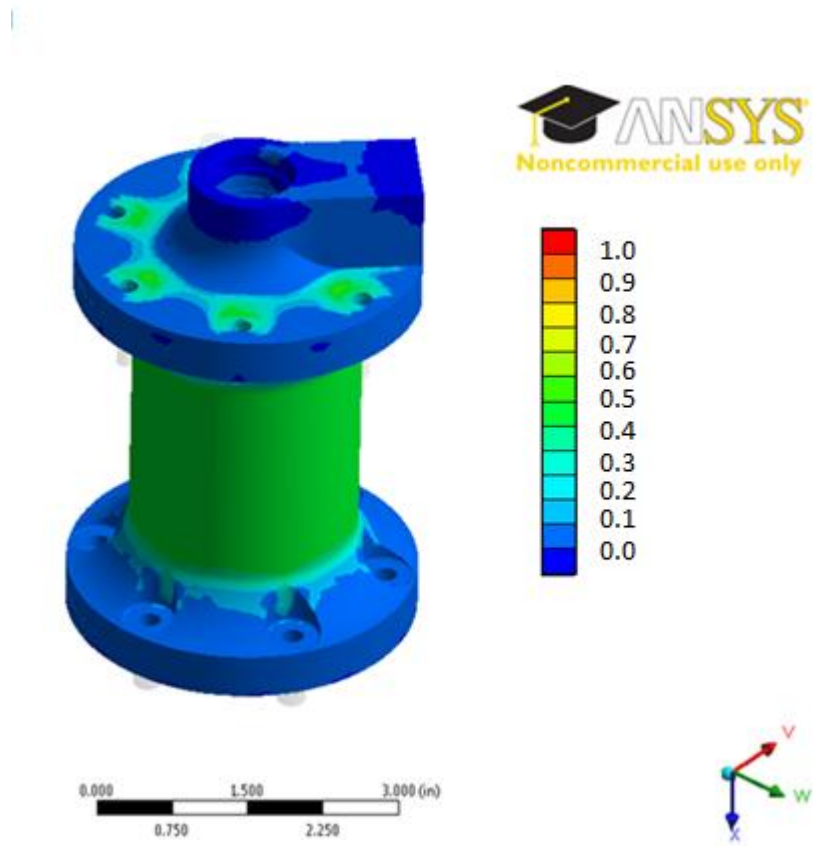


Figure 15 Von mises equivalent stress for enclosure parts of bonded contact FEA under proof loading(full)



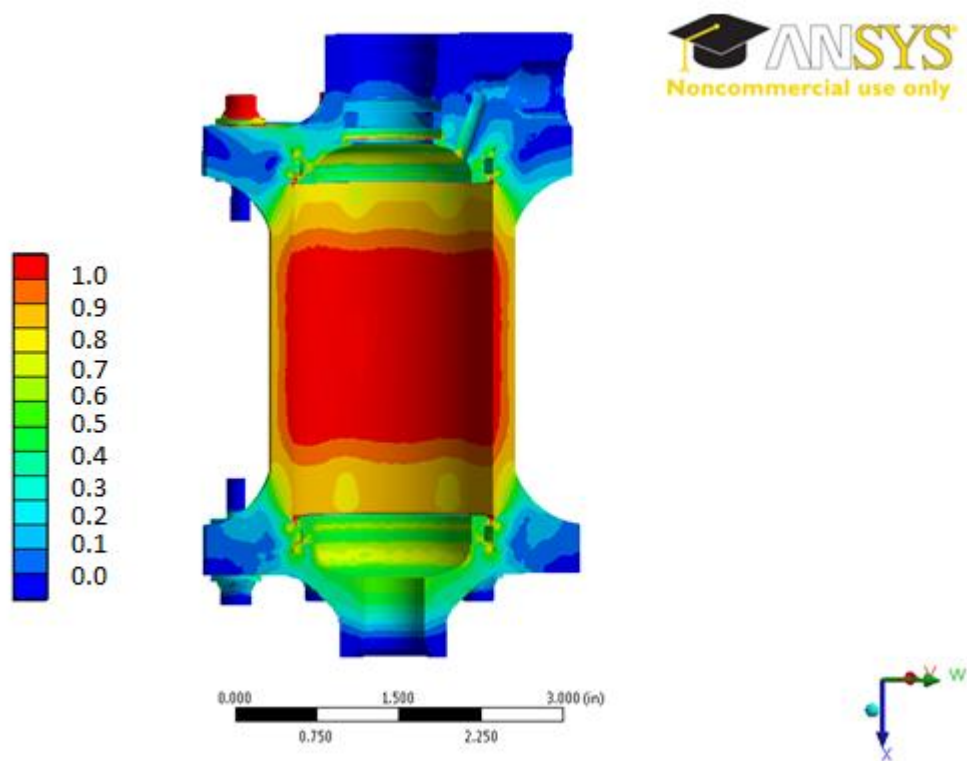


Figure 16 Von mises equivalent stress for enclosure parts of bonded contact FEA under proof loading (cross-section)

## 5. Finite Element Analysis of Piston Assembly

There are three loading modes for the piston;

- Tension
- Compression
- Buckling
- Mechanical bonding

The first three can be easily studied by finite element analysis. The last one requires actual testing because there is not enough information regarding the helicoil insert that will be chosen by injection molding vendor. For simplicity piston is studied by itself rather than being integrated with enclosure parts and proper boundary conditions are applied. The Finite Element study of piston is divided in two parts; Proof Loading and Work loading. Furthermore this study under Proof and Work load consists of three subdivisions of piston being; fully contracted, halfway and fully extended.

### 5.1.Geometry

Geometry is made in UGS N.X. 7.0. For simplicity and reduction in calculation effort bushings are removed and instead their contact area is marked for a proper boundary condition as shown in Figure 17. Since only buckling of TORLON part is of interest Rodend, locknut, washer, helicoil insert and O-seal are excluded in FEA. Also, detail features such as threads and glue hole are taken out as well.

Next three configurations are made based on the position of the piston in actuator;

- Fully contracted: where piston head bottoms out against the Back Cover and piston rod bushing (marked grey in Figure 17) is farthest from piston head bushing.
- Half way: piston is in half stroke and piston rod bushing is positioned in the middle of the piston rod.
- Fully extended or full stroke: where piston head bottoms out against the Front Cover.

Volume is divided in three segments for applying boundary conditions. Then geometry is imported into ANSYS 12.1.



Figure 17 From left to right; Fully contracted, Half way and Fully extended

## 5.2.Mesh

Once the geometry was imported into ANSYS, the automatic mesh module was used for meshing due to complicated geometry. Mesh metric reported for the three geometries are described as;

- Contracted; 66, 683 elements with average Jacobian ratio of 3.29 and standard deviation of 1.3.
- Half way; 66,612 elements with average Jacobian ration of 3.29 and standard deviation of 1.33.

- Extended; 66,344 elements with average Jacobian ratio of 3.29 and standard deviation of 1.33.

In all three cases mesh has been made by standard mechanical and with Tet10 (Solid187) and Hex20 (Solid186) which are a 10 node Tetrahedron (ANSYS 12.1 Element Reference Manual, 2009) and 20 node hexahedron (ANSYS 12.1 ELEMENT Reference Manual, 2009) respectively. Both of these elements have degrees of freedom in UX, UY and UZ only. Figure 18 demonstrates the automatic meshes generated in ANSYS 12.1.

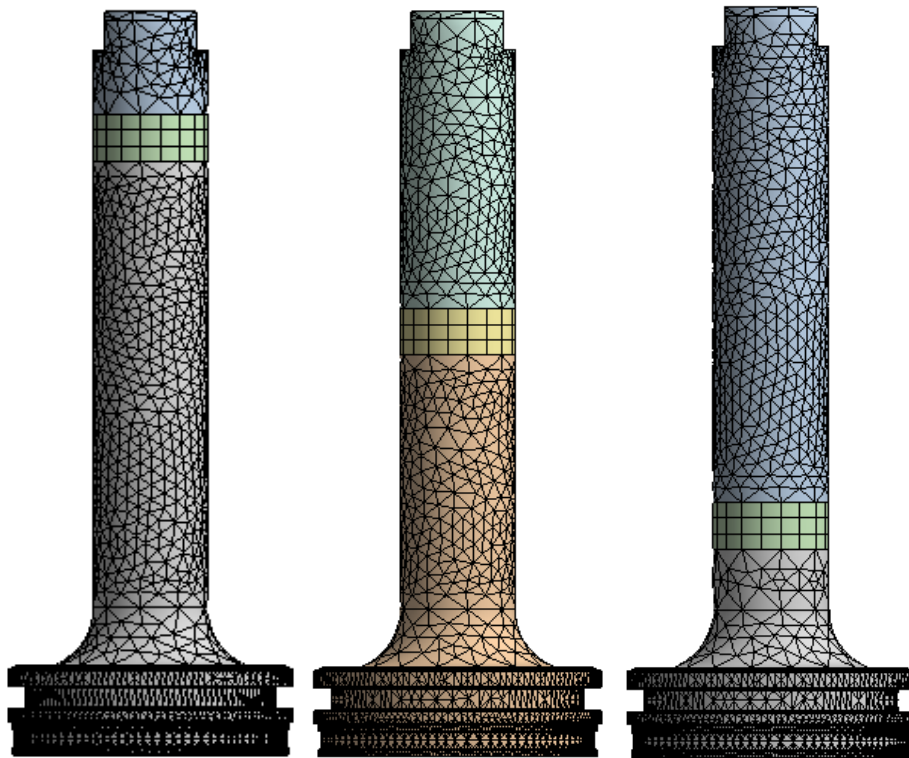


Figure 18 Mesh for the piston, from left to the right; contracted, halfway and fully extended with average jacobian ration of 3.29, 3.29 ,3.29

### 5.3.Loads and Boundary conditions for compression mode

After the meshing was completed loads and boundary conditions were applied. Note that at a given time under operation, the actuator is pressurized on both side of the piston assembly (on OD of piston and ID of the piston). To further simplify the analysis and also due to fairly symmetric loading

(beside the small difference between the surface area above and under piston head) when pressure is applied it is applied as psi difference.

Since configurations are the same for all three cases load and boundary conditions applied are the same for all three cases. Boundary conditions are shown in Figure 19 and they are described below;

- Rodend location: free in radial direction and fixed in axial for washer face and all faces inside the Rodend hole.
- Piston rod bushing: fixed in radial direction and free in axial are applied to the segment of piston rod surface where the piston bushing is located.
- Piston head bushing: fixed in radial direction and free in axial are applied to the surface that contact with ID of the cylinder or the bushing. Since O-seal is squishy it is assumed that the surface that bushing makes contact with is free to move.

Figure 20 demonstrates how loads are applied. There are two loads;

- Pressure which applied to the bottom of the piston and all interior of the piston rod weight relief cut.
- Side load which is applied to one of the “wrench grab” faces as a pressure. The surface area of wrench grab face was obtained by ANSYS to be  $0.10363 \text{ in}^2$  which makes the  $30\text{lb}_f$  side load to have an equivalent pressure of 289psi.

Thermal load is dropped out of the analysis. In radial direction piston is pushing against the O-seals and bushing which are squishing compared to rigidity of Torlon 5030 and also there is no thermal mismatch since Front Cover and Cylinder are made out of the Torlon 5030 as well. In axial direction piston can expand freely. Thus thermal expansion does not cause any major stress on the piston.

■ RodEnd: Free in radial, Fixed in axial  
 Components: Free, 0, Free in

■ Bushing: Free in axial, Fixed in radial  
 Components: 0, Free, 0, in

■ PistonHead: Free in axial, Fixed in radial  
 Components: 0, Free, 0, in

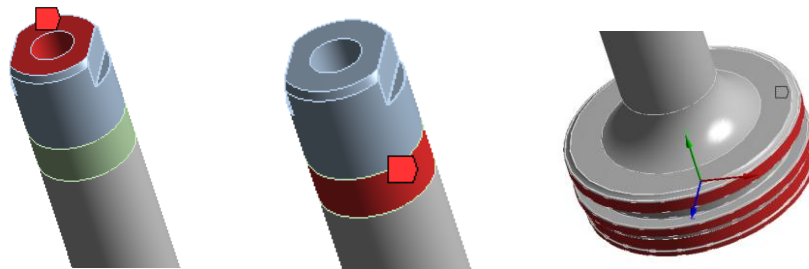


Figure 19 Boundary conditions for the piston in compression mode and buckling

■ Pressure: 2130. psi
 ■ SideLoad: 289. psi



Figure 20 Loads for the piston in compression mode and buckling

#### 5.4.Loads and Boundary conditions for tension mode

Since the actuator under goes a cyclic motion of pulling and pushing, it is subject to both compression and tension. Piston goes to tension mode when actuator goes from fully extended toward contracted mode. In tension mode pressure is applied to the exterior faces of the piston in which are inside the enclosure parts. Thus the OD of piston rod sees the most amount of pressure when actuator is nearly in full contraction.

The magnitude of pressure in tension mode is equal to compressive mode. On the other hand the boundary condition and implemented pressure loads are applied differently. The boundary condition at piston head and piston bushing stay constant but the boundary condition changes as shown in Figure 21. Since piston undergoes a uniform tension at the washer face there are no displacement constraints. Thus mechanical bonding is completely subjected to the rod end thread-helicoil and helicoil-Torlon thread strength.

The driving pressure is applied to the OD of the piston rod and top of the piston head as shown in Figure 22. The 30lb<sub>f</sub> side load is applied in the same way that it was applied in compressive mode. Since the geometry used in this part of the analysis is the same as piston fully contracted for compressive mode the mesh remains the same. For details please refer to the previous section, 5.2 Mesh.

- RodEnd: Free in radial, Fixed in axial  
 Components: Free, 0, Free in
- Bushing: fixed in radial, free in axial  
 Components: 0, Free, 0, in
- PistonHead  
 Components: 0, Free, 0, in

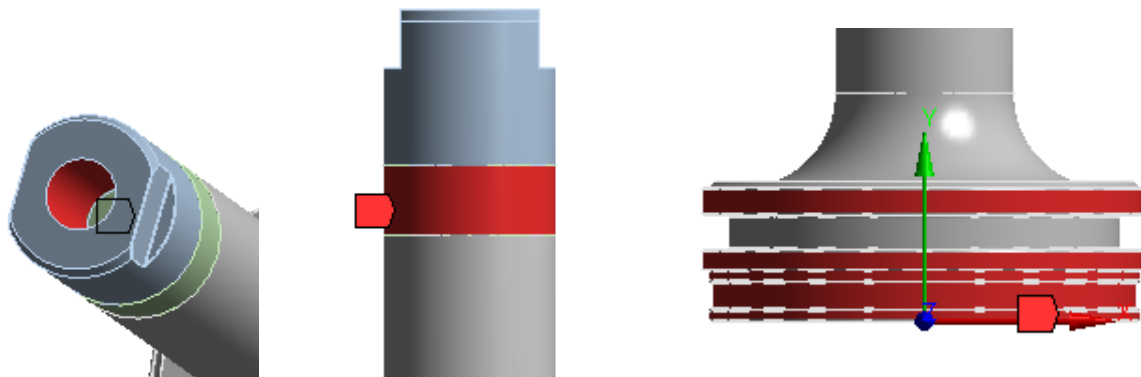


Figure 21 Boundary conditions for the piston in tension mode

- Pressure: 2130. psi
- SideLoad: 289. psi



Figure 22 Loads for the piston in tension mode



### 5.5.Solver's Algorithm for buckling

The buckling approach done here is a linear buckling for calculating the first mode which is the most critical one. Nonlinear buckling analysis is not applicable here since the geometry is close to a simple cantilever beam. Nonlinear buckling analysis is more appropriate for cases where there is stress stiffening and there are significant prebuckling rotations. An example of such a structure can be a slender arched beam where structure experiences a sudden snap (Cook, 2002).

The FEA buckling analysis consists of two parts. Part one which a static structural analysis where the stiffness matrix is determined. Part two in which the solver uses an algebraic eigenvalue method that gives the buckling modes (eigenvalues);

$$[K]\{d\} = 0$$

Where  $K$  is the net stiffness and to be precise it consists of bending stiffness and geometric stiffness matrix;

$$K = [K_B - \lambda K_G]$$

Therefore none trivial solutions of equation above are of interest. This means values of  $\lambda$  for which  $K$  is a singular matrix (Accorsi, 2011).

### 5.6.Compression mode stress evaluation

Before Buckling Analysis was performed the structure needed to be pre-stressed. This means applying the compressive loads and the proper boundary conditions to the piston assembly, section 5.3. Once the static structure analysis was complete, results were post processed for the three piston-actuator modes (Fully contracted, Half way and Fully extended mode).

The Von Mises stress contours for the piston under proof loading is shown for the three cases;

- Contracted mode, Figure 23.
- Half way mode, Figure 24.
- Fully extended mode, Figure 25.

Notice there is a small difference in stress trend for each piston-actuator mode. This is due to the fact that boundary conditions are different for each piston-actuator mode. The purpose of this table is to highlight the maximum stress at critical locations of interest. Again, stress on all areas is kept below 5ksi. The maximum stress occurs on the piston rod radius.

Another important feature of this design is incorporating the dome shape optimization for the piston head. Note that stress in piston head at the dome is 60 percent of stress in piston. This is due to the shape optimization done to obtain the optimized factor for the ratio of dome height to dome ID (25%). The shape optimization is explained in Section 7 Stress Reduction by shape optimization.

There are areas in the contour plot of Von mises stress that have stresses which are not realistic. For example there are high stresses due to discontinuity where different bodies meet. The geometry was sectioned in order to be able to generate mapped mesh which yields elements that have Jacobian ratio closer to 1. However since sectioning geometry produces discontinuity, it causes unrealistic stress jumps. An example this where body sectioned for the piston rod bushing meets the mating bodies of piston rod. There are also singularities at sharp edges and corners such as the bottom of the rod end hole. Unfortunately there is very little that can be done to remove these singularities to better capture the stress other than further refining the mesh which is computationally expensive. However these locations are not of special interest and therefore it is safe to ignore them.

A side from discontinuities and singularities which makes the contour plots of the stress somewhat not realistic and unintuitive, there are poisson ratio contractions on both side of the location of the body for the piston rod bushing and also where there is a sudden change in thickness of mating bodies under a uniform stress. For example refer to the Figure 23 Von mises stress for the piston under proof loading in contracted mode. There two areas where area on the ID of the piston rod that have stresses higher than midsection of ID of the piston rod. This is due to fact that at each end of these two areas the thickness is higher which causes poisson contraction.

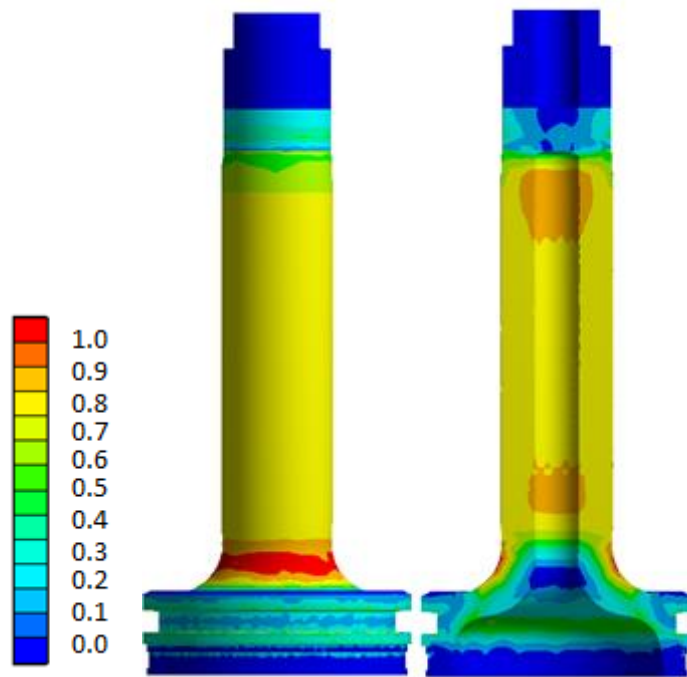


Figure 23 Von mises stress for the piston under proof loading in contracted mode

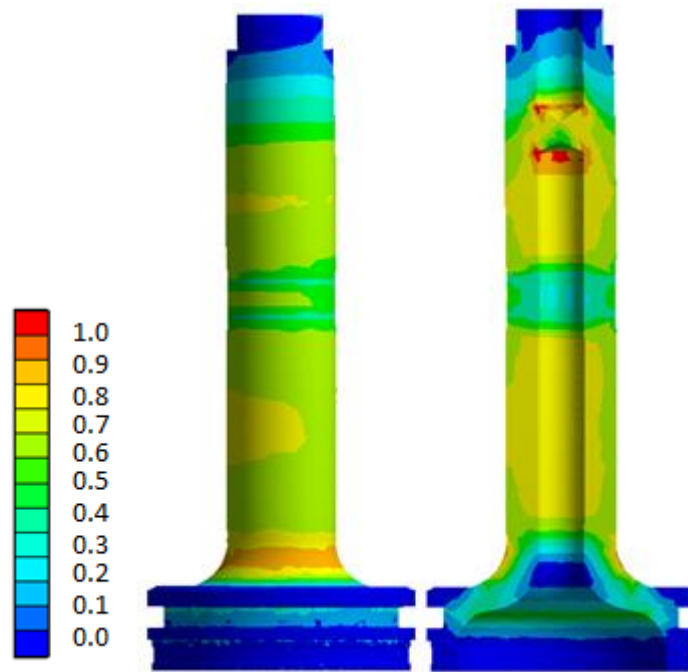


Figure 24 Von mises stress for the piston under proof loading in half way mode

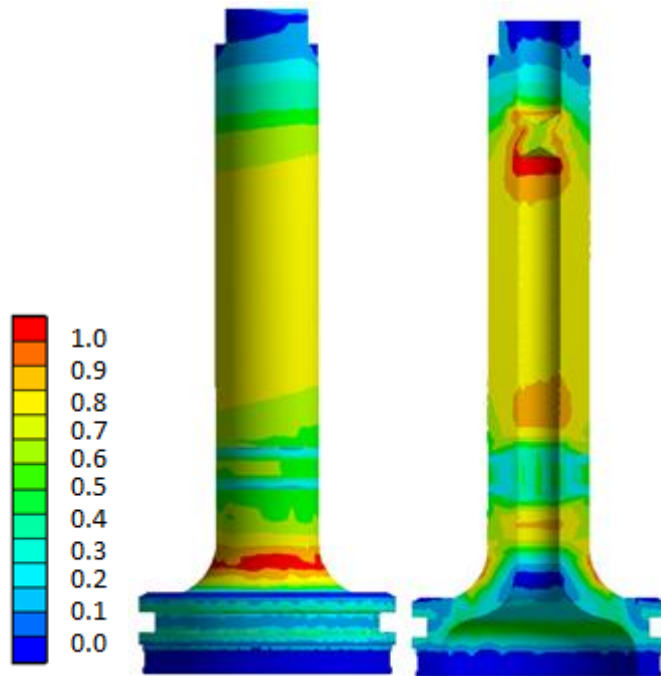


Figure 25 Von mises stress for the piston under proof loading in fully extended mode

### 5.7. Piston assembly under buckling

Once eigenvalue problem was solved by ANSYS, eigenvalues were extracted. Since it was predicted that first mode of the buckling is the most critical one, the first eigenvalue represents the critical buckling load factor. These buckling load factors for all three loading conditions are listed in Table 4. Since the actual loads were applied as reference loads these buckling load factors have somewhat of an interpretation of a safety load factor. For example as Table 4 shows for the fully

extended mode the buckling load factor is 3.76 under proof loading. This means piston can be loaded by 3.76 times of proof pressure and side load before it buckles (ANSYS 12.1 Linear Buckling, 2009). Note that piston is most susceptible to buckling when it is fully extended and it is strongest against buckling when it is located in half way stroke which agrees with hand calculation in Section **Error! Reference source not found. Error! Reference source not found..** This is because the column buckling length for extended mode is largest for the fully extended case. In order to better understand the deflection of the piston, the exaggerated mode shape for the first mode of the piston under buckling for the three cases of; contracted, half way and fully extended is shown in Figure 26. This figure demonstrates an intuitive check for mode shape comparison of the three cases of contracted, half way and extended.

Loading	Contracted	Half way	extended
Proof	8.8972	146.3	3.760
Work	26.474	435.2	11.191

Table 4 Buckling load factor for proof and working loading

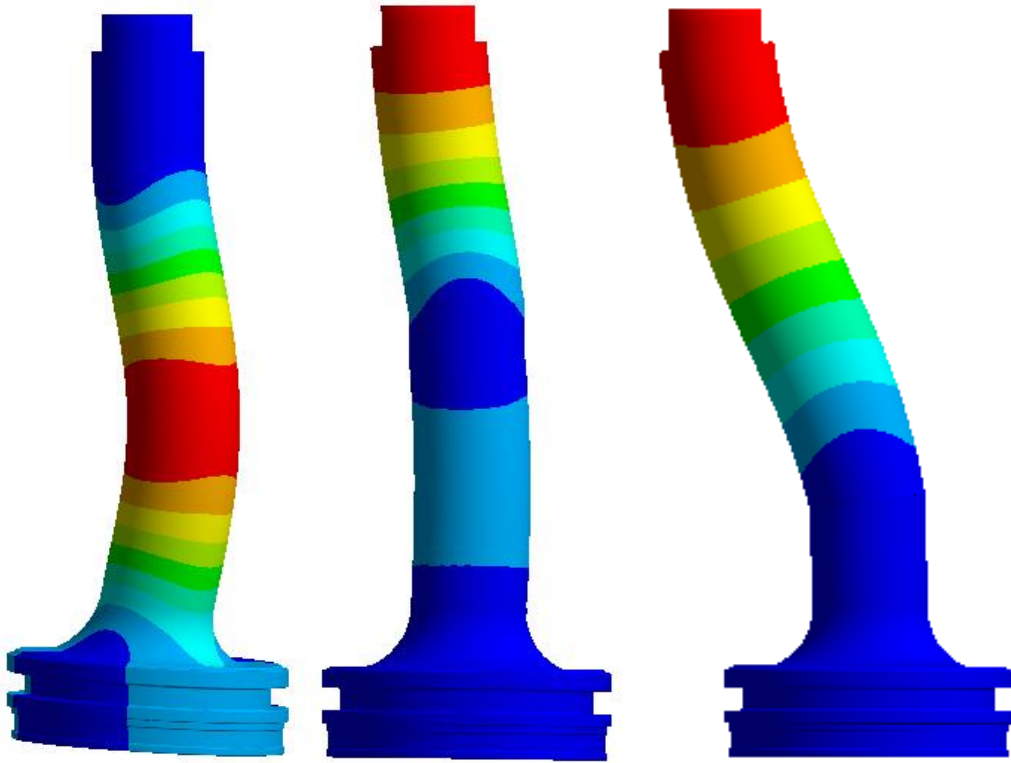


Figure 26 exaggerated modal displacement for proof loading: from left to right; Fully contracted, Half way and Fully extended

### 5.8. Tension mode stress evaluation

Once the meshing and applying the loads and boundary conditions were complete the same static structural analysis as in compressive mode was used to obtain the state of stress in piston, Section 5.5 Solver's . Figure 27, shows the Von Mises stress for piston in tension mode under Proof loading. As it is demonstrated stress is somewhat similar to piston in compression mode for fully contracted case as expected. The small difference in stress level is due to the fact that indeed boundary conditions and surface area in which pressure is applied are different between the two cases. The maximum stress occurs on piston rod ID.



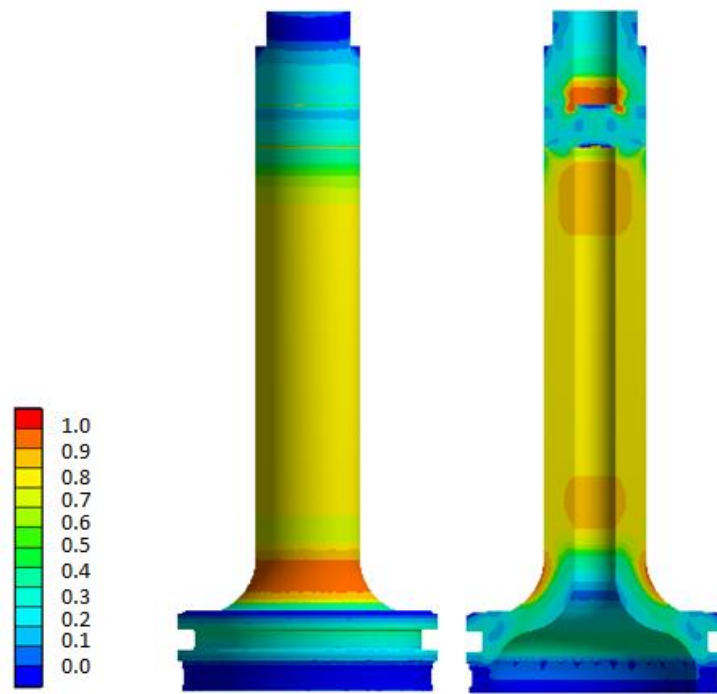


Figure 27 Von mises stress for piston in tension mode under proof loading

## 6. Failure Criteria

In order to confirm that the composite-made Actuator can function as well as the current Aluminum-made actuator a series failure criteria has been considered and the functionality of Actuator under proof and working loading has been considered. Before starting the discussion about failure analysis it is important to mention the assumptions that has been made;

- The material property of TORLON 5030 is assumed to be Isotropic since the fibers are very small (about 1/32”) and are randomly oriented. The manufacturer of TORLON 5030, *Solvay Advance Polymers*, provided the isotropic-linear elastic property of TORLON 5030 which can found in Table 1. These properties are taken from *Torlon Design Guide Manual* which is last updated in June 2010.
- Based on specification provided by *the sponsor of this program it was assumed more than 98% of the time the Actuator is under normal work loading. The work loading pressure is noted to be 211 psid. However the actuator must be designed in a way that can withstand the proof loading under special circumstances such as pump malfunction. These specifications are mentioned in section 1.4 Specifications page 6. Therefore when considering the proof loading a smaller factor of safety was considered under proof loading.*
- The effect of water absorption, surface wear and induced fracture is not considered at this point in the project. The purpose of this section is to predict via FEA and analytical approach whether TORLON 5030 can be used as structural polymers with significant weight savings. The effects mentioned above are addressed separately in section 10. Risk Assessment page 53.

Once these assumptions are made a Finite Element code is written in ANSYS 12.1 to look at the failure criteria such as Static Structural, Buckling, Creep, Impact and Fatigue. The result of FEA is

examined by analytical solution for sanity check. The details and results of these analyses are discussed in following sub sections.

### **6.1. Static Structural**

After running the simulations in ANSYS it is concluded that the highest stress occurs in piston rod radius and cylinder ID in midsections. However these values are kept below 5ksi. Now looking at the Torlon Design Guide Manual (Solvay Advance Polymers, 2003) tensile strength of Torlon 5030 at 275°F is reported to be 23.1 ksi. Looking at the highest stress these parts it is clear that actuator operates at safe zone.

### **6.2. Buckling**

Before discussing the buckling it is important to understand the loading cases in conjunction with buckling itself. A side from the mathematical description, buckling in practice is characterized by a sudden failure of a structural member subjected to high compressive stress, where the actual compressive stress at the point of failure is less than the ultimate compressive stresses that the material is capable of withstanding (Shigley, 2006). Even though under normal working conditions the maximum stress is below 1ksi it is important to prevent the piston from buckling from the highest compressive load that happens for Proof loading regardless of the fact that the actuator must be built so that it can withstand the Proof loading for the case of unexpected compressor surge load. The reason for this precaution is because it takes only one surge load to buckle the piston and once buckled, piston fails.

After running the buckling analysis and confirming it with hand calculation it is clear that piston is most susceptible to buckling when it's in extended mode under proof loading. A summary of buckling load factors is shown in Table 4. When in extended mode under proof loading, the associated buckling load factor is 3.76. This means under a compressor surge load actuator can withstand 3.76 times of its proof load before the piston buckles.

When in normal working condition the piston is well designed to be safe from buckling. Table 4 shows that under normal working condition and in fully extended mode, the buckling load factor is 11.1.

One important note is the reason why the order of buckling load factor from highest to lowest follows; halfway mode, fully contracted mode and fully extended mode. When in fully extended mode piston buckling length is highest. However for fully extended mode piston boundary conditions are such that on rod end side it is free and on piston head end it is pinned (or to be conservative and safe it's fixed). Versus for fully contracted mode boundary conditions are pinned-pinned. When piston is in halfway mode it has the smallest buckling length and the boundary conditions at worse is pinned-free just like fully extended mode.

It is critical to realize that cylinder for this design concept is not susceptible to buckling. This is due to the way the actuator is mounted. Since this actuator is designed to be mounted to a plate by its front cover, it is free to expand in axial direction. This actuator can be clevis mounted and the cylinder won't be susceptible to buckling however it is ever mounted in a way that it is constrained on both front cover and back cover it can undergo buckling.

### 6.3. Creep

Unlike buckling, creep highly depends on time in which structure is held on at certain loads. Thus actuator is most susceptible to creep during cruise loading because more than 98% of its life in service it operates under work loading. Fortunately stresses induced by work loading are below 5ksi. According to the Figure 4 creep resistance performance of TORLON 5030 at 400°F at 5ksi and 10ksi for 1,000 hours is zero. Thus actuator is well protected against creep since the operating temperature for the actuator is 300°F.

## 6.4.Fatigue

When analyzing fatigue it is highly important to recognize the exact frequency and stress in which a structure is operating within that range. For this actuator it is assumed that piston oscillates back and forth with a frequency of 1 Hz under normal operating conditions. By shape optimization the maximum stress for work loading was kept below 1ksi and for proof loading less than 5ksi. Figure 28 shows the fatigue performance of TORLON 5030 at 350°F and 30Hz. (Solvay Advance Polymers, 2003). Thus extracting from the Figure 28 the actuator can withstand Proof loading less than  $1.5 \times 10^6$  cycles and work loading  $1.0 \times 10^9$  cycles. Note that these values are the number of cycles at a load case alone. This means if it is desired to estimate the total fatigue life an actuator, one must track number of cycles for occurrence of each loading. In other words the fatigue life of the actuator is not simply  $1.5 \times 10^6 + 1.0 \times 10^9$ . Another important key is that Figure 28 is the fatigue at 350°F and 30Hz, the actuator operates at a maximum operating temperature of 300°F and 1Hz which could mean higher fatigue life. However this must be verified by conducting the fatigue test at 300°F and 1 Hz.

---

## High Temperature Flexural Fatigue Strength of TORLON Resins at 350°F (177°C), 30Hz

---

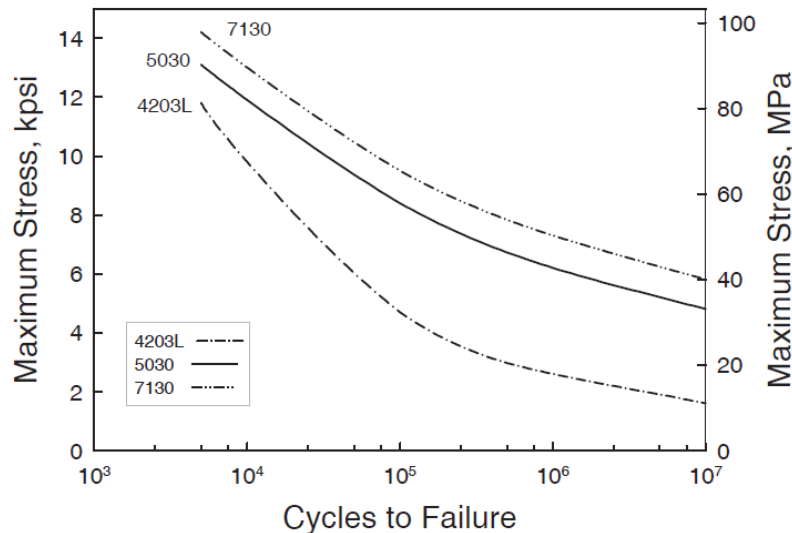


Figure 28 High temperature flexural fatigue strength of TORLON resin at 350F, 30Hz

## 7. Stress Reduction by shape optimization

After researching through catalogs of plastics it was realized that there are not many high temperature plastics that could replace Aluminum. In fact Torlon 5030 has a slightly lower specific strength than Aluminum does. However the current progress in technology exclusively speaking in CAD and FEA allows engineers to perform design optimization to improve their design by reducing the stress. After taking a closer look at the current Actuator a first CAD models were built in UGS NX 7.0 and the FEA code in ANSYS Mechanical APDL 11.1 was built to look at the structural performance of the Actuator.

Since the Actuator resembles more or less of a pressure vessel stress reduction can be done to places such as end caps and flange because these places have complex geometry. Calculating the stress in cylinder is easily obtained by a simple thin/thick wall formula for pressure vessel and it was expected

that there will not be significant amount of stress reduction there. At the time our ANSYS had licensing restrictions we were limited to only 250K nodes. Thus a simple 2D axisymmetric model with PLANE42 element was built. These models were built as the progress of defining the best configuration was done.

The first model was done similar to the current design and the only difference is the method of attachment, for our case being glued. Figure 29 shows the state of stress in first model. Notice the color band has been modified to show the stress corresponding to failure limit of TORLON 5030( $\pm 30$ ksi). From the result of the first model it was concluded that the Front/Back Cover sees the most amount of stress. After series of 12 iterations the optimized shaped of Front/Back Cover was obtained. The optimized Front/Cover was concluded to be domed shape with a dome height to dome ID ratio of 0.25 and it resulted in reducing the stress by a factor of 10 as shown in Figure 30. Also, this result shows that flange mount Front/Back Cover configuration results in lower stresses as well.

Once the optimized dome parameter for the Front/Back Cover was obtained, the Academic Research License for ANSYS was purchased to investigate the stress level in 3D. By doing so the right thickness and radius for more details such as Hydraulic In/Out, Piston rod opening, flange radius and back-spot-faces was obtained.

1

NODAL SOLUTION

STEP=1

SUB =1

TIME=1

/EXPANDED

SEQV (AVG)

DMX =.015782

SMN =454.033

SMX =163787



OCT 4 2011

09:59:40

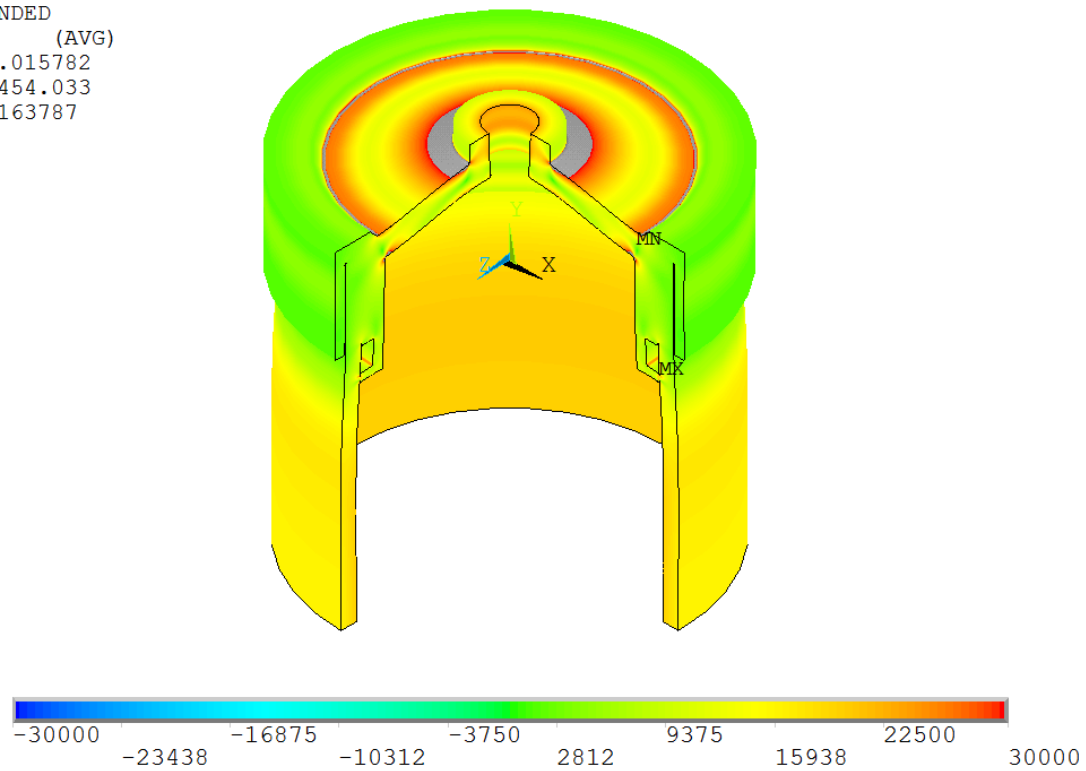


Figure 29 First simplified 2D model with flat Front/Back Cover in glued on configuration demonstrating the stress in endcap being 156ksi at 2130psi



1  
NODAL SOLUTION  
STEP=1  
SUB =1  
TIME=100  
/EXPANDED  
SEQV (AVG)  
DMX =.035953  
SMN =207.085  
SMX =88761

  
Noncommercial use only  
OCT 4 2011  
10:05:15

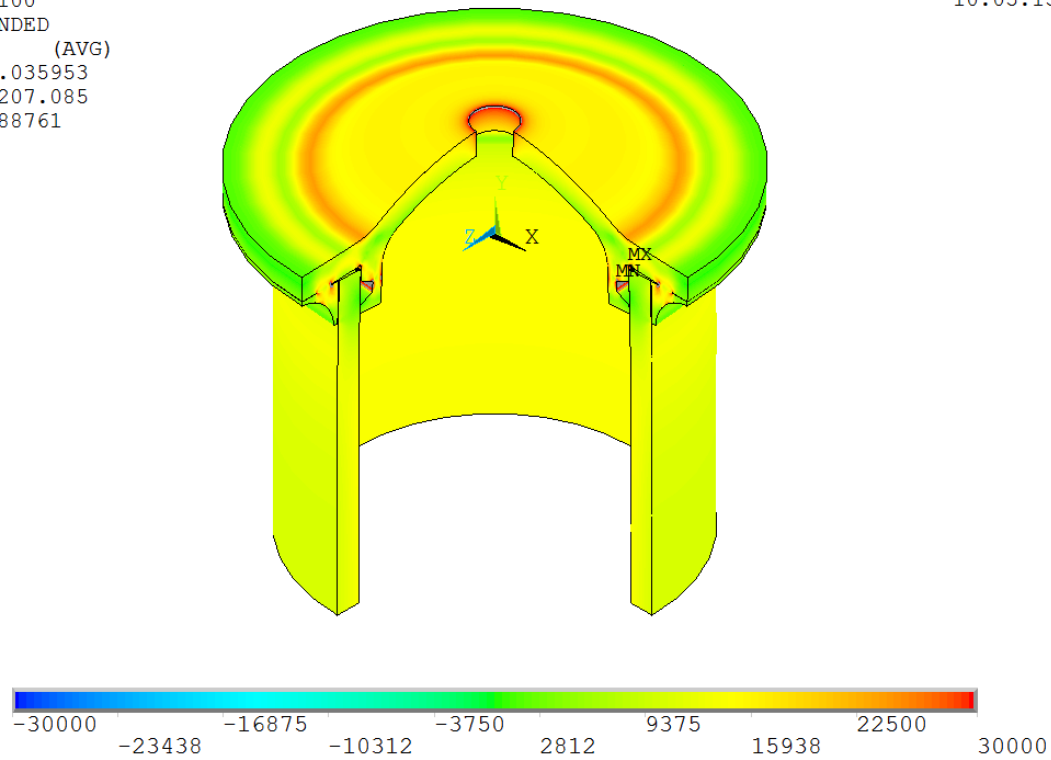


Figure 30 Optimized dome shaped Front/Back Cover in flange mount configuration with highest stress being 22.5ksi at 2130psi

## 8. Weight Decrease by shape optimization

The current aluminum actuator that has the same load rating as the one redesigned in this project weighs about 5.65 lbs. This is including the weight of the LVDT that is missing in TORLON actuator. The TORLON actuator was designed as a proof the concept of composite actuator and adding LVDT was outside of the scope of this project. Adding the LVDT feedback is merely replacing the Back Cover with a something close to Front Cover that has hydraulic inlet angled 90 degrees to the side and adding the LVDT opening. The LVDT by itself weighs about 0.1 to 0.3 lb.

The TORLON actuator weighs about 1.4lbs. This includes the weight of all washer, bolts, nuts and O-rings and only excludes the weight of the LVDT. The weight reduction brings in 400% weight savings in

total. Note, the reason the TORLON actuator weighs 4 times less than the aluminum actuator is because of the shape optimization done through 12 iterations of FEA integrated with CAD. The specific strength of the Aluminum is higher than TORLON 5030 at all temperatures. Therefore one must realize the key winning in success of this project for weight saving is not simply TORLON 5030, but more importantly Aluminum weighs less than TORLON 5030 for the same strength.

Part	QTY	Weight(lb)
Front Cover	1	0.199
Back Cover	1	0.145
Cylinder	1	0.490
Piston Assembly	1	0.133
N10 Bolts	12	0.130
N10 Nut	12	0.056
N10 Washer	24	0.030
5/16 Lock Nut	1	0.015
5/16 Washer	1	0.001
Bushing	2	0.003
Orings	9	0.013
Scraper	1	0.001
Fittings	2	0.130
Rod End	1	0.058
Heilcoil	1	0.005
<b>NET WEIGHT (lb)</b>		<b>1.409</b>
<b>CURRENT ACTUATOR (lb)</b>		<b>5.650</b>
<b>WEIGHT SAVINGS(%)</b>		<b>401</b>

Table 5 Complete part list with weights and weight savings for TORLON actuator

## 9. Manufacturing Cost Savings

As mentioned above once shape optimization was done to the perfection, stress and weight of the design reduced by a factor of 10 and 4. Then we took advantage of injection molding capabilities of the TORLON 5030 to further increase the benefits of this project by eliminating manufacturing costs associated to machining.

The process of fabricating the current Aluminum actuator involves enormous amount of machining a block of aluminum to the size, tolerance and specified surface finish. Furthermore all hydraulic in/out

lets and mounting bases must be welded in place. Thus the major capital cost of the current aluminum actuator comes from labor.

The injection molding of TORLON eliminates this major cost in labor. When redesigning the current actuator it was realized that beside piston rod OD, Cylinder ID and the piston rod opening on the front cover there are no other critical tolerance and surface finish that is not achievable by injection molding (Solvay Advance Polymers, 2003). Once the mold design for TORLON 5030 is perfected injection molding of TORLON can yield tolerance and surface finish as well as 0.001" and 16 microns.

Unfortunately in order to be able to take the part out of the mold a draft angle of  $\frac{1}{2}^{\circ}$  to  $1^{\circ}$  to the added to certain faces, in the case of actuator to Cylinder ID and Piston OD for all other places a split mold can be used. However we have been able to detour around this obstacle by adding small amount of extra thickness (0.001" to 0.003") to the draft angle surfaces around grind them down to the specified tolerances and surface by post machining.

The manufacturing cost of the TORLON actuator is quoted by AZTEC, Inc, a potential vendor that has successfully molded the piston to the specified dimension, tolerance and surface finish for this project. The price quote from AZTEC is shown in Figure 31. As it's shown the injection mold for the Cylinder costs the most. This is due to the size of the Cylinder. It is worth to mention that the cost of the injection molding of TORLON increases dramatically with the size of the part. Any complex shape can be molded to at least nearest net shape which can reduce major labor costs.

Once all costs are identified, a simple cost analysis is done to calculate the pay back. Table 6 shows the cost analysis for the TORLON actuator. The net cost of a TORLON actuator for an estimated annual usage(EAU) of 3000 parts per year is \$233.60 per actuator. This includes the cost of all molded parts, none molded parts and post machining costs. The cost of the current aluminum actuator is \$3000. Therefore production cost saving is 92%. This means for an estimated annual usage of 3000 parts per

year the net manufacturing cost saving for the first year is \$8.183M with the payback of selling only 96 parts. After the first year the total manufacturing cost savings would be \$8.299M. Notice that besides manufacturing cost savings there is another profit gained by reducing the weight per hour of flight. Since the cost per hour of a flight for both commercial and military applications was not provided by Hamilton Sundstrand the weight reduction savings is not calculated here. However this saving can easily be calculated as;

$$\text{Cost saving per hour of flight} = (4.241\text{lb}) \times (\text{number of actuator per aircraft}) \times (\text{cost per pound-hour})$$

### Quote by Aztec Plastic Company

Injection Molding

Case Hardened Steel Mold

EAU of 3,000

#### Back Cover

Tooling: \$25,000.00  
Each: \$23.00

#### Cylinder

Tooling: \$47,000.00  
Each: \$60.00

#### Piston Assembly

Tooling: \$14,000.00  
Each: \$22.60

#### Front Cover

Tooling: \$30,000.00  
Each: \$28.00



Figure 31 Injection molding quote for TORLON parts presented by Aztec Plastic, Inc.

<b>EAU</b>	<b>3000</b>
Molded parts	\$133.60
Post Machining	\$50.00
None Molded parts	\$50.00
Molding Investment	\$116,000.00
Net Cost	\$233.60
Current Cost	\$3,000.00
production savings per part	92%
1st year savings	\$8,183,200.00
Savings After 1st year	\$8,299,200.00
Payback (parts to be sold)	96

Table 6 Cost analysis for TORLON actuator based on 3,000EAU

## 10. Risk Assessment

No different from other high saving projects, this project has risks that need to be addressed. The most serious one is surface wear. Surface wear occurs at moving parts such as piston rod OD and piston rod opening on front cover. Surface wear can potentially cause the hydraulic fluid to leak.

Second biggest risk is exposure to moisture so far. It is known that water gets absorbed by most polymers and TORLON 5030 has small volumetric change and strength drop due to water absorption (Solvay Advance Polymers, 2003). However it is believed that eventually water absorption will stabilize. In order to proof this concept a water test is suggested.

### 10.1. Surface Wear

The biggest risk associated with moving parts is wear. In the actuator piston moves back and forth with a frequency of approximately 1Hz. There are two loads affecting the wear;

1. Working pressure of the actuator that causes swelling of piston which exerts pressure on the ID of the cylinder and also on the front cover-piston opening.
2. Side load of 30lbf when the actuator is in full stroke.

The result of FEA shows the how much pressure is exerted as a result of swelling.

The side load is most catastrophic when actuator is in full stroke. Figure 32 shows the side load and reaction forces. There are only two equilibrium equations and there are five unknown reaction forces which makes this problem statically indeterminate. However under the assumption that all loads are carried by bushings until bushings are not worn out we can find the reaction forces to be; 89.3lbf and 119.3lbf for Piston Head Bushing ( $F_{PHB}$ ) and Piston Rod Bushing ( $F_{PRB}$ ) respectively. Once these forces are known the nominal stress exerted on the bushing can be obtained by;

$$nomial\ stress = \frac{F}{projected\ area}$$

Which yields pressures to be 72.4 psi and 169.7 psi Piston Head Bushing ( $P_{PHB}$ ) and Piston Rod Bushing ( $P_{PRB}$ ) respectively. Table 7 shows the projected surface area for parts subjected to wear which was obtained by;

$$Project\ surface\ area = h \times 2\pi r$$

Where h is the axial length of part and r is the radius of the part subjected to wear.

Another parameter for wear beside pressure is the velocity at which surfaces are rubbed against each other. As suggested by the sponsor the actuator should be tested for a velocity of maximum 300% of full stroke in 1 second. In terms of linear velocity;

$$v = 3 \times (stroke) \times \frac{1}{frequency}$$

Which is 11.8 inches per seconds or 57 Feet Per Minutes (FPM).

Most industries characterize wear as Pressure multiplied by Velocity ( $pv$ ). Taking  $P_{PRB}$  as the control limit,  $pv$  for this particular actuator can said to be about 9,673 psi-fpm. Unfortunately there are no test data or literature on wear properties of TORLON 5030 against a bushing material or any metal making it impossible to predict whether TORLON 5030 can withstand this  $pv$ .

Although wear is a complicated matter and there are many variables controlling the wear one can forecast the likely hood of wear being a project killer. Here we have listed why we think wear may not be an issue.

Wear of two mating surfaces are the worst if the two surfaces are made of the same material. As long as we can find a bushing material that wears at a higher rate than TORLON 5030 then we can schedule maintenance to replace the bushings. This way moving parts made out of TORLON 5030 will never rub against each other.

One objection that was raised by the sponsor was that the glass fibers in TORLON 5030 after machining will stick out and eat away the bushing very quickly. This will not likely be the case because the “glass fibers” in TORLON 5030 are more like glass powder (average fiber length 1/32”). In the process of molding there will be about 0.003” excess resin left on draft angle surfaces such as Piston Rod and ID of Cylinder that will be grinded down during post machining. The surface finish obtained by grinding the ID of Cylinder and Piston Rod are in 6-9 micron range. Also, the hardness of TORLON 5030<sup>1</sup> is less than Al 2024<sup>2</sup> by only 20%. Even though there are no guarantees for TORLON 5030 to have wear properties similar to Al2024 at least to major contributors are close to current material for actuator.

Another way of dealing with wear surfaces that completely eliminates the wear of TORLON 5030 is by metalizing wear surfaces. Currently chromium plating is an applicable way of metalizing polymers. Another advantage of metalizing is eliminating the water absorption by TORLON 5030. Of course there are issues such as metalizing the interior surfaces, delamination due to thermal mismatch and cost effectiveness of the process that need further research and time investment.

---

<sup>1</sup> 97 Brinell 10mm steel ball 500kg converted (Depot, 2010) from 94 Rockwell E (Solvay Advance Polymers, 2003)

<sup>2</sup> 120 Brinell 10mm steel ball 500kg (MatWeb, 2010)



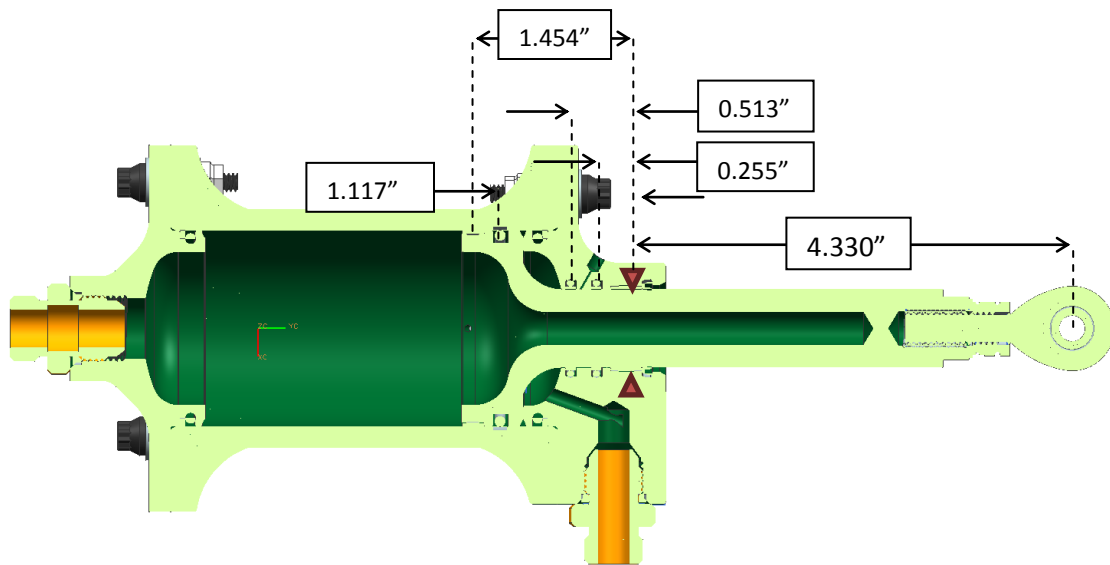


Figure 32 Actuator in full stroke

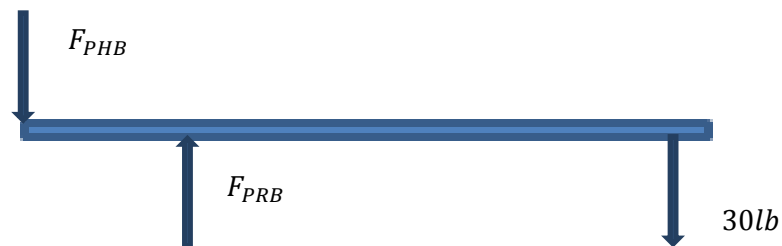


Figure 33 Force equilibrium diagram on piston for calculating the reaction forces caused by the side load

Piston Head Bushing	Piston Rod Bushing	Slipper Band on Piston Head O-ring Seal	Slipper Band on Piston Rod O-ring Seal
1.234 in <sup>2</sup>	0.703 in <sup>2</sup>	0.819 in <sup>2</sup>	0.224 in <sup>2</sup>

Table 7 Projected surface area for parts subjected to wear

## **10.2. Water absorption**

If the actuator is operating in humid condition it will be exposed to water absorption. While operating the temperature of the actuator reaches as high as 300°F. It is not clear whether exposure to moisture would cause significant degradation.

There are limited water absorption data provided by the manufacturer of TORLON. Once fully saturated with water at room temperature there is a 1.6% Weight increase however there is no data regarding the strength of TORLON 5030 due to water absorption. The only data so far is 7% drop in tensile strength of the TORLON 4203L after it is saturated in water at room temperature. TORLON 4203L is the resin with no reinforcement.

Only 7% drop in tensile strength is not catastrophic, the highest stress in TORLON actuator at Proof loading is 5ksi. However these results need to be verified for absorption of water at 300°F. As mentioned in previous sub section, one way to prevent the actuator from degradation due to water would be metalizing the interior of the actuator. Another way would redesign the actuator to the specified saturated properties of TORLON 5030. This would literally mean increasing the thickness of the walls.

## **11. Summary**

The design of the composite actuator is constrained to creep performance of the resin material. There are not many high temperature resin materials that are commercially available. TORLON 5030 is identified as a high temperature glass filled short fiber composite that is applicable for this particular project. The injection moldability of TORLON 5030 is an advantage for eliminating the manufacturing costs associated with machining for the current aluminum made actuator.

After considering different design concepts it is concluded that an actuator with removable end caps and short bolts would have the smallest amount of creep and best accessibility for maintenance.

The result of the FEA revealed that piston experiences the highest stress among the other parts and it occurs at piston radius. However the Von Mises stress at this critical location is kept below 5ksi. Based on failure analysis the design limiting failure criteria is fatigue. According to TORLON 5030 fatigue curve at 350°F and 30Hz fatigue life for 2 loading cases of Proof and Work loading are  $1.5 \times 10^6$  and  $1.0 \times 10^9$  cycles respectively. However it is proposed that fatigue data be generated at 300°F and 1Hz.

There are risks associated with this new technology such as water absorption and surface wear. It is recommended that a material characterization test be done on the TORLON 5030 to quantify the degradation due to water absorption for TORLON 5030 and also characterize the surface wear.

All together the injection moldable composite actuator with detailed drawing and tolerances was designed within one year. Aztec plastic is selected as the potential vendor and a quote for injection molding tooling cost for production was obtained and the first prototype was built in addition of six months. Figure 34 shows the 1<sup>st</sup> prototype. The piston is injection molded, the cylinder is machined from an extruded rod and covers are machined from aluminum due to low budget.

The key winning aspect of this project is design optimization via CAD integrated with FEA. This enabled shape optimization which yielded a weight reduction of factor of 4 and stress reduction of factor of 10. Further carefully selecting a high temperature performance injection moldable plastic eliminated major manufacturing cost in machining which is estimated to be 92 percent.

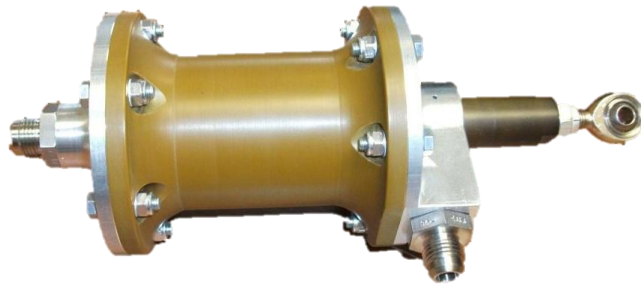


Figure 34 The prototype TORLON actuator. Cylinder is machined from extruded TORLON rod, Piston is injection molded. Front and Back Cover are machined from Aluminum due to low budget.

## Work Cited

- Accorsi, M. (2011). CE-5164 Finite Element I. *Lecture on Buckling*.
- ANSYS 12.1 ELEMENT Reference Manual. (2009). *SOLID186*. SAS IP, Inc.
- ANSYS 12.1 Element Reference Manual. (2009). *SOLID187*. SAS IP, Inc.
- ANSYS 12.1 Linear Buckling. (2009). Linear Buckling Analysis. //Mechanical (formerly Simulation) // The Mechanical Application Approach // Analysis Types // Linear Buckling Analysis. SAS IP, Inc.
- Cook, M. P. (2002). *Concepts and applications of finite element analysis*. Hoboken, NJ: Wiley.
- Depot, C. (2010, 01 01). *Hardness Conversion Chart*. Retrieved from Carbide Depot:  
<http://www.carbidedepot.com/formulas-hardness.htm>
- Gibson, R. F. (1994). *Principles of composite material mechanics*. McGraw-Hill.
- Jones, R. M. (1975). *Mechanics of composite materials*. Hemisphere Publishing Corps.
- MatWeb. (2010, 01 01). *ASM MATWEB*. Retrieved from  
<http://asm.matweb.com/search/SpecificMaterial.asp?bassnum=MA2024T4>
- RCF Technologies, J. C. (2010, 05). <http://www.rcftechnologies.com/>. Retrieved from  
<http://www.rcftechnologies.com/>.
- Shigley. (2006). *Mechanical Engineering Design*. McGraw-Hill.
- Solvay Advance Polymers, L. (2003). *Torlon Polyamide-imide Design Guide*. Alpharetta, GA: Solvay.